

## One-way photoisomerization of ligands for permanent switching of metal complexes

Andrey G. Lvov,<sup>1,2,3</sup> Max Mörtel,<sup>1</sup> Frank W. Heinemann,<sup>1</sup> Marat M. Khusniyarov<sup>1\*</sup>

<sup>1</sup>Department of Chemistry and Pharmacy, Friedrich-Alexander University Erlangen-Nürnberg (FAU), Egerlandstrasse 1, 91058 Erlangen, Germany, e-mail: [marat.khusniyarov@fau.de](mailto:marat.khusniyarov@fau.de)

<sup>2</sup>A.E. Favorsky Irkutsk Institute of Chemistry, Siberian Branch of the Russian Academy of Sciences, 1 Favorsky St., 664033 Irkutsk, Russia

<sup>3</sup>Irkutsk National Research Technical University, 83 Lermontov St., 664074 Irkutsk, Russia

### Table of contents

<b>I. General Information .....</b>	S2
<b>II. Examples of previously isolated DAE-a isomers (literature overview).....</b>	S3
<b>III. NMR and ESI-MS spectra for L-a.....</b>	S4
<b>IV. X-ray Crystallography .....</b>	S6
<b>V. Cyclic Voltammetry .....</b>	S13
<b>VI. Magnetic Measurements .....</b>	S14
<b>VII. Mössbauer Spectroscopy .....</b>	S23
<b>VIII. Photochemistry .....</b>	S26
<b>VIII.1. NMR studies .....</b>	S27
<b>VIII.2. Electronic absorption spectroscopy .....</b>	S32
<b>IX. DFT Calculations .....</b>	S36
<b>X. References .....</b>	S58

## I. General Information

**Materials.** All starting materials and solvents were utilized as received without further purification unless otherwise noted. Pure anhydrous solvents were collected from a solid-state solvent purification system Glass Contour (Irvine, CA). Toluene Uvasol® for preparative photolysis and photochemical studies was purchased from Supelco® and degassed by “freeze-pump-thaw” procedure (3 times). Diarylethene **L-0** was prepared according previously reported procedure.<sup>1</sup>

**Instrumentation.** Elemental analyses were carried out with a EURO EA analyzer from EuroVector. NMR spectra were recorded with JEOL ECX 400 MHz, JEOL ECP 400 MHz and JEOL EX 270 MHz in rotating 5 mm o.d. tubes and processed with *Delta V4.0* software provided by JEOL Ltd. High-resolution mass spectra were obtained with a Bruker maXis TM UHR-ESI-TOF mass spectrometer.

## II. Examples of previously isolated DAE-a isomers (literature overview)

**Table S1.** Literature-known examples of **DAE-o** → **DAE-a** conversion.

No	Year [ref]	Reaction scheme ( <b>DAE-o</b> → <b>DAE-a</b> )	mDAE-o (c)*	mDAE-a†	Yield
1	2008 [ <sup>2</sup> ]		- (5 mM)	-	26%
2	2015 [ <sup>3</sup> ]		149 mg (1.4 mM)	34 mg	23%
3	2015 [ <sup>4</sup> ]		5 mg (0.86 mM)	0.2 mg	4%
4	2015 [ <sup>5</sup> ]		20 mg (0.09 mM)	3.4 mg	17%
5	2017 [ <sup>6</sup> ]		150 mg (1.6 mM)	15 mg‡	10%
6	2020 [ <sup>7</sup> ]		105 mg (2.7 mM)	31 mg	30%
7	2020 [ <sup>8</sup> ]		18 mg (0.48 mM) 12 mg (0.32 mM)	7.1 mg 2.4 mg	43% 25%

\*Weight of the parent **DAE-o** isomer used in photolysis experiment (concentration).

† Weight of isolated **DAE-a** photoisomer.

‡ Only one isomer was isolated.

### III. NMR and ESI-MS spectra for L-a

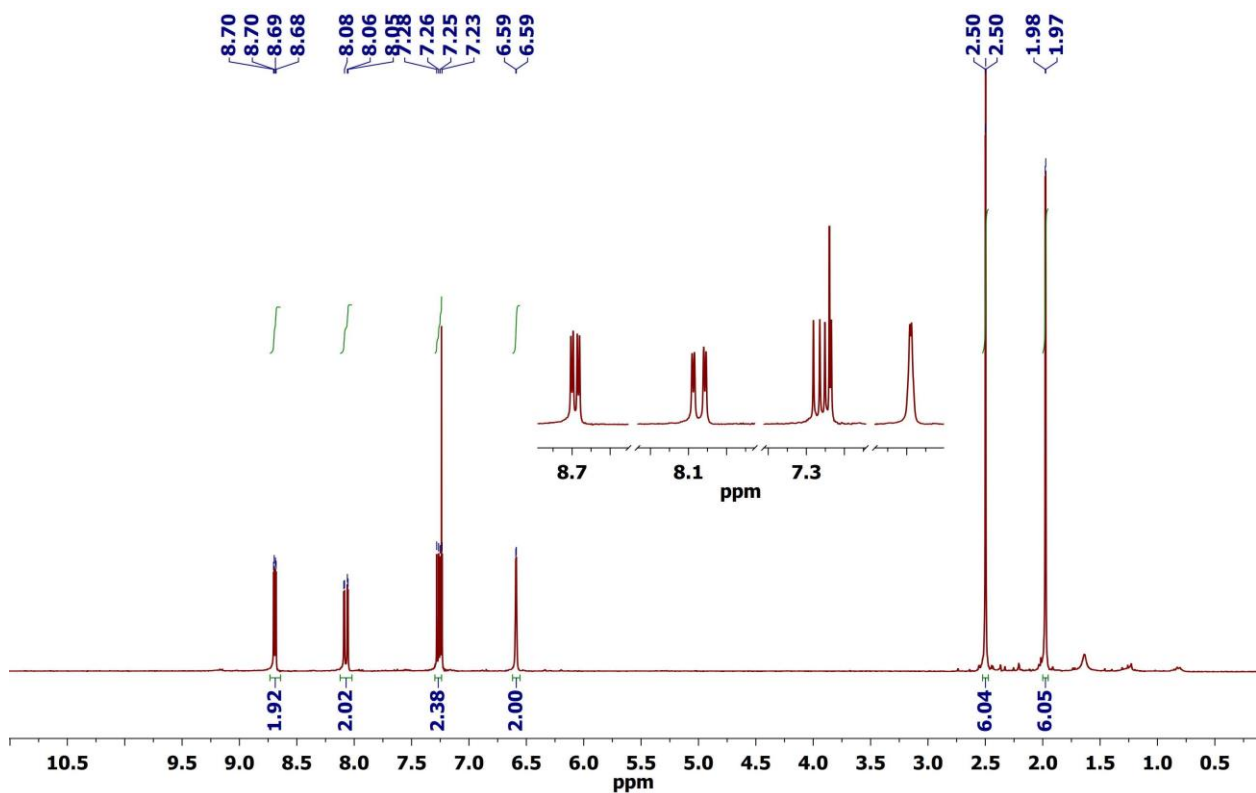


**Figure S1.** <sup>1</sup>H NMR spectrum of L-a ( $\text{CDCl}_3$ ).

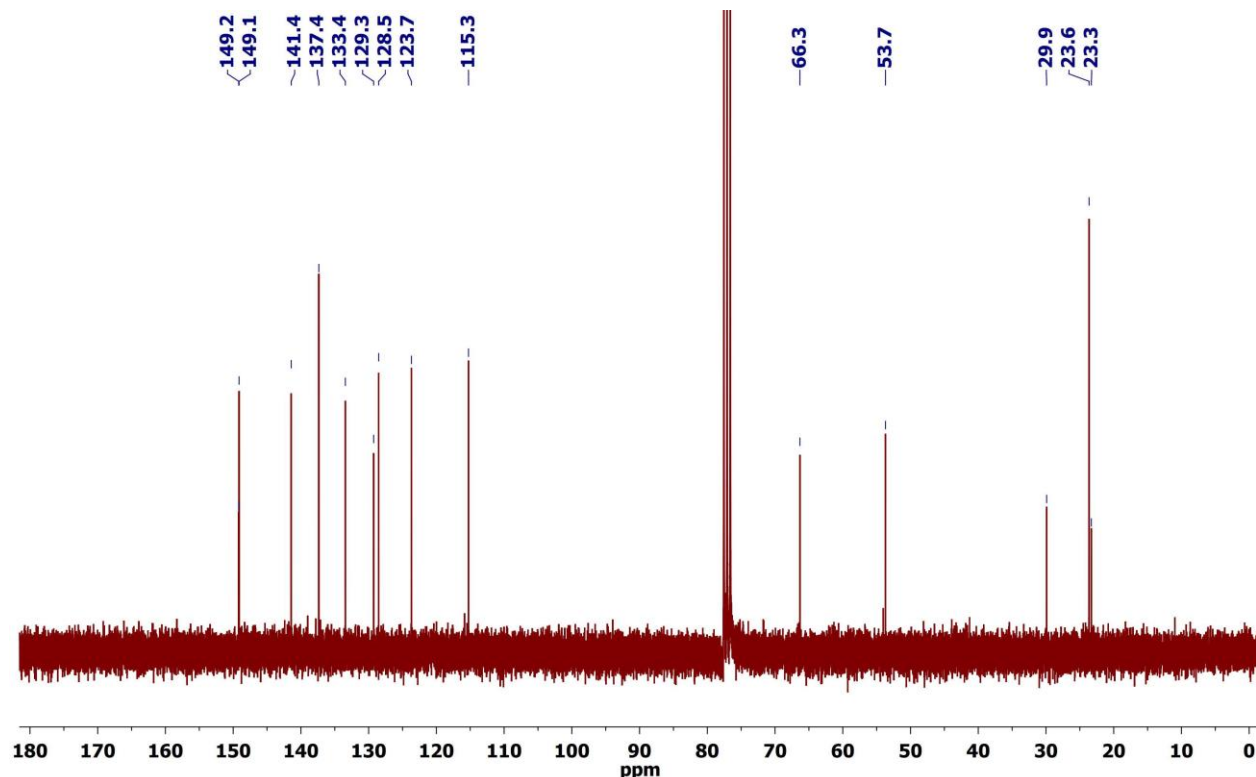


**Figure S2.** <sup>13</sup>C NMR spectrum of L-a ( $\text{CDCl}_3$ ).

Sample Name	AGR-88	Instrument	maXis	255552.10137
Comment	tune low positive mode in MeCN			

**Acquisition Parameter**

Source Type	ESI	Ion Polarity	Positive	Set Nebulizer	0.4 Bar
Focus	Active	Set Capillary	3400 V	Set Dry Heater	180 °C
Scan Begin	50 m/z	Set End Plate Offset	-500 V	Set Dry Gas	4.0 l/min
Scan End	1250 m/z	Set Charging Voltage	0 V	Set Divert Valve	Waste
		Set Corona	0 nA	Set APCI Heater	0 °C

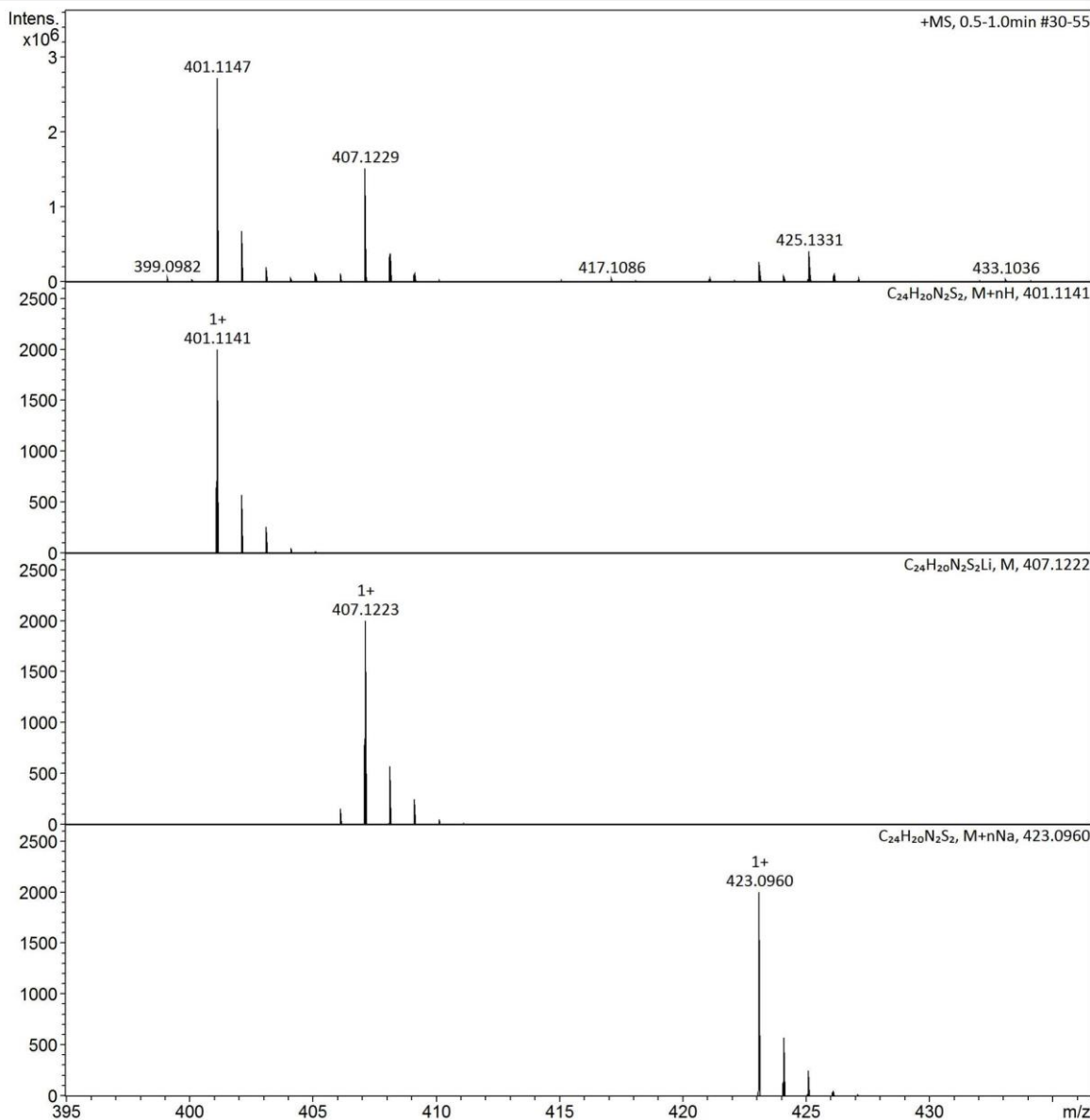


**Figure S3.** ESI-MS spectrum of L-a.

#### IV. X-ray Crystallography

**Crystallographic information:** CCDC-2035356 (for **L-a**), 2035357 (for **1-a** at 100 K), and 2035358 (for **1-a** at 273K) contain the supplementary crystallographic data for compounds **1-8**, respectively, in this paper. The data can be obtained free of charge from The Cambridge Crystallographic Data Centre via [www.ccdc.cam.ac.uk/structures](http://www.ccdc.cam.ac.uk/structures).

Suitable crystals were embedded in protective perfluoropolyalkyl ether oil and transferred to the cold nitrogen gas stream of the diffractometer. Intensity data were collected for **L-a** at 100 K, for **1-a** at 100 and 273 K using MoK $\alpha$  radiation ( $\lambda = 0.71073 \text{ \AA}$ ) on Bruker Kappa PHOTON 2  $I\mu S$  Duo diffractometer equipped with QUAZAR focusing Montel optics. Data were corrected for Lorentz and polarization effects, and semiempirical absorption corrections were performed on the basis of multiple scans using SADABS.<sup>10</sup> The structures were solved by direct methods (SHELX XT 2014/5)<sup>11</sup> and refined by full-matrix least-squares procedures on  $F^2$  using SHELXL 2018/3.<sup>12</sup> All non-hydrogen atoms were refined with anisotropic displacement parameters. With the exception of the water hydrogen atoms in **L-a**, all hydrogen atoms were placed in positions of optimized geometry, and their isotropic displacement parameters were tied to those of the corresponding carrier atoms by a factor of either 1.2 or 1.5. Crystallographic data, data collection, and structure refinement details are given in Table S2.

**Details for L-a.** The molecule was disordered. Two alternative orientations were refined and resulted in site occupancies of 66.9(9) and 33.4(9) % for the affected atoms S1, S2, C1, C3 and S1A, S2A, C1A, C3A, respectively. The compound crystallized with one molecule of H<sub>2</sub>O per formula unit. The positions of the water hydrogen atoms were taken from a difference Fourier synthesis and their positional parameters were refined. Note, that the observed disorder is not due to **L-o** or **L-c** impurities, but due to two possible orientations of methyl groups at photoactive carbon atoms relative to the mean ligand plane: up-down and down-up.

**Details for 1-a at 100K.** The molecule was disordered. Two alternative orientations were refined and resulted in site occupancies of 51.2(6) and 48.8(6) % for the affected atoms S1, S2, C21, C23 and S1A, S2A, C21A, C23A, respectively. The compound crystallized with two molecules of toluene per formula unit.

**Details for 1-a at 273K.** The crystal structure undergoes a temperature dependent phase transition. In this high temperature, monoclinic phase the molecule is situated on a crystallographic twofold rotation axis (Wyckoff position 2e), while in the low temperature triclinic phase **1-a** at 100K the molecule is situated on a general position. The molecule was disordered. Two alternative orientations were refined and resulted in site occupancies of 50 % each for the affected atoms S1, C11, C13 and S1A, C11A, C13A, respectively. The compound crystallized with two molecules

of toluene per formula unit. The independent toluene molecule was also disordered. Two alternative orientations were refined and resulted in site occupancies of 52.2(7) and 47.8(2) % for the atoms C101–C107 and C111–C117, respectively. Similarity restraints were applied to the anisotropic displacement parameters of the atoms of the toluene molecule.

**Table S2.** Crystallographic data, data collection, and structure refinement details.

	<b>L-a·H<sub>2</sub>O</b>	<b>1-a·(C<sub>7</sub>H<sub>8</sub>)<sub>2</sub></b> (100 K)	<b>1-a·(C<sub>7</sub>H<sub>8</sub>)<sub>2</sub></b> (273 K)
CCDC	2035356	2035357	2035358
Temperature, K	100(2)	100(2)	273(2)
Chemical formula	C <sub>24</sub> H <sub>22</sub> N <sub>2</sub> OS <sub>2</sub> (C <sub>24</sub> H <sub>20</sub> N <sub>2</sub> S <sub>2</sub> · H <sub>2</sub> O)	C <sub>50</sub> H <sub>52</sub> B <sub>2</sub> FeN <sub>10</sub> S <sub>2</sub> (C <sub>36</sub> H <sub>36</sub> B <sub>2</sub> FeN <sub>10</sub> S · (C <sub>7</sub> H <sub>8</sub> ) <sub>2</sub> )	C <sub>50</sub> H <sub>52</sub> B <sub>2</sub> FeN <sub>10</sub> S <sub>2</sub> (C <sub>36</sub> H <sub>36</sub> B <sub>2</sub> FeN <sub>10</sub> S · (C <sub>7</sub> H <sub>8</sub> ) <sub>2</sub> )
Formula weight	418.55	934.60	934.60
Crystal system	tetragonal	triclinic	monoclinic
Space Group	<i>I</i> 4 <sub>1</sub>	<i>P</i> -1	<i>C</i> 2/c
<i>a</i> , Å	21.4320(9)	13.2188(8)	18.0723(7)
<i>b</i> , Å	21.4320(9)	13.3326(8)	20.5790(7)
<i>c</i> , Å	8.9094(5)	13.6012(8)	13.5331(5)
$\alpha$ , deg	90	100.534(2)	90
$\beta$ , deg	90	96.772(2)	107.072(2)
$\gamma$ , deg	90	100.648(2)	90
<i>V</i> , Å <sup>3</sup>	4092.4(4)	2287.4(2)	4811.3(3)
Z	8	2	4
$\rho_{\text{calcd}}$ , g·cm <sup>-3</sup>	1.359	1.357	1.290
$\mu/\text{mm}^{-1}$	0.279	0.470	0.447
F(000)	1760.0	980.0	1960.0
Crystal Size, mm	0.25 × 0.12 × 0.1	0.3 × 0.24 × 0.22	0.3 × 0.24 × 0.22
Radiation	MoKα ( $\lambda = 0.71073$ )	MoKα ( $\lambda = 0.71073$ )	MoKα ( $\lambda = 0.71073$ )
2θ range for data collection/°	3.8 to 57.4	4.064 to 56.57	3.958 to 55.75
Index ranges	-28 ≤ <i>h</i> ≤ 28, -26 ≤ <i>k</i> ≤ 28, -12 ≤ <i>l</i> ≤ 12	-17 ≤ <i>h</i> ≤ 17, -17 ≤ <i>k</i> ≤ 17, -13 ≤ <i>l</i> ≤ 18	-23 ≤ <i>h</i> ≤ 23, -27 ≤ <i>k</i> ≤ 27, -17 ≤ <i>l</i> ≤ 17
Reflections collected	75840	81250	80308
Independent reflections	5299 [ $R_{\text{int}} = 0.0909$ , $R_{\text{sigma}} = 0.0330$ ]	11332 [ $R_{\text{int}} = 0.0446$ , $R_{\text{sigma}} = 0.0283$ ]	5701 [ $R_{\text{int}} = 0.0577$ , $R_{\text{sigma}} = 0.0232$ ]
Data/restraints/ parameters	5299/4/309	11332/0/629	5701/237/350
Goodness-of-fit on <i>F</i> <sup>2</sup>	1.056	1.096	1.120
Final R indexes [ $I >= 2\sigma(I)$ ]	$R_1 = 0.0467$ , $wR_2 = 0.1079$	$R_1 = 0.0499$ , $wR_2 = 0.1215$	$R_1 = 0.0585$ , $wR_2 = 0.1393$
Final R indexes [all data]	$R_1 = 0.0513$ , $wR_2 = 0.1108$	$R_1 = 0.0607$ , $wR_2 = 0.1289$	$R_1 = 0.0845$ , $wR_2 = 0.1613$
Largest diff. peak/hole / e Å <sup>-3</sup>	0.29/-0.27	0.88/-0.46	0.33/-0.29

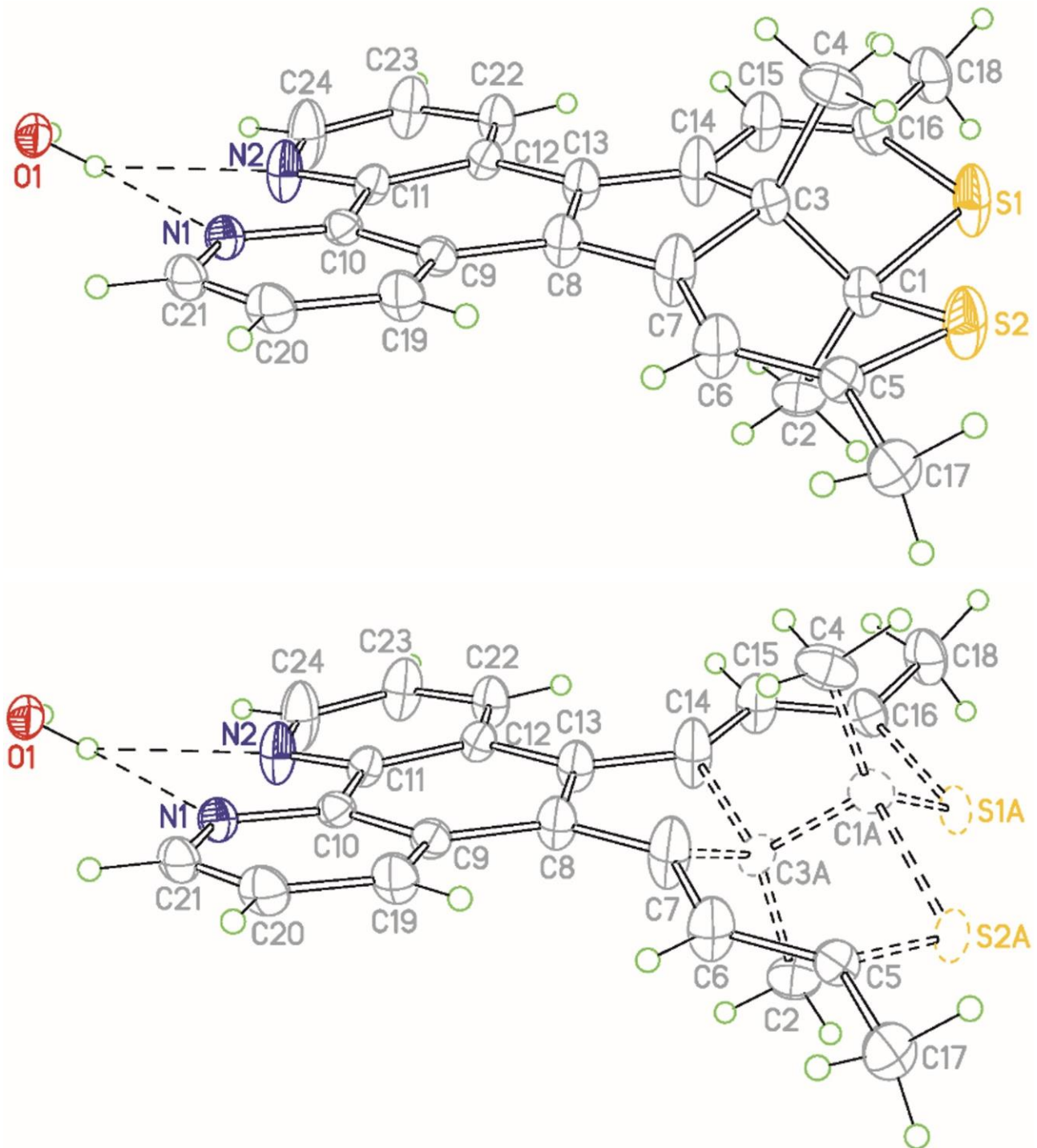


**Figure S4.** Solid-state molecular structure with the applied numbering scheme for **L-a** @ 100 K in crystals of **L-a·H<sub>2</sub>O**. Thermal ellipsoids are drawn at the 50% probability level. The two alternative orientations of the disordered molecule are presented (site occupancies are 66.6(9) % (top) and 33.4(9) % (bottom)).

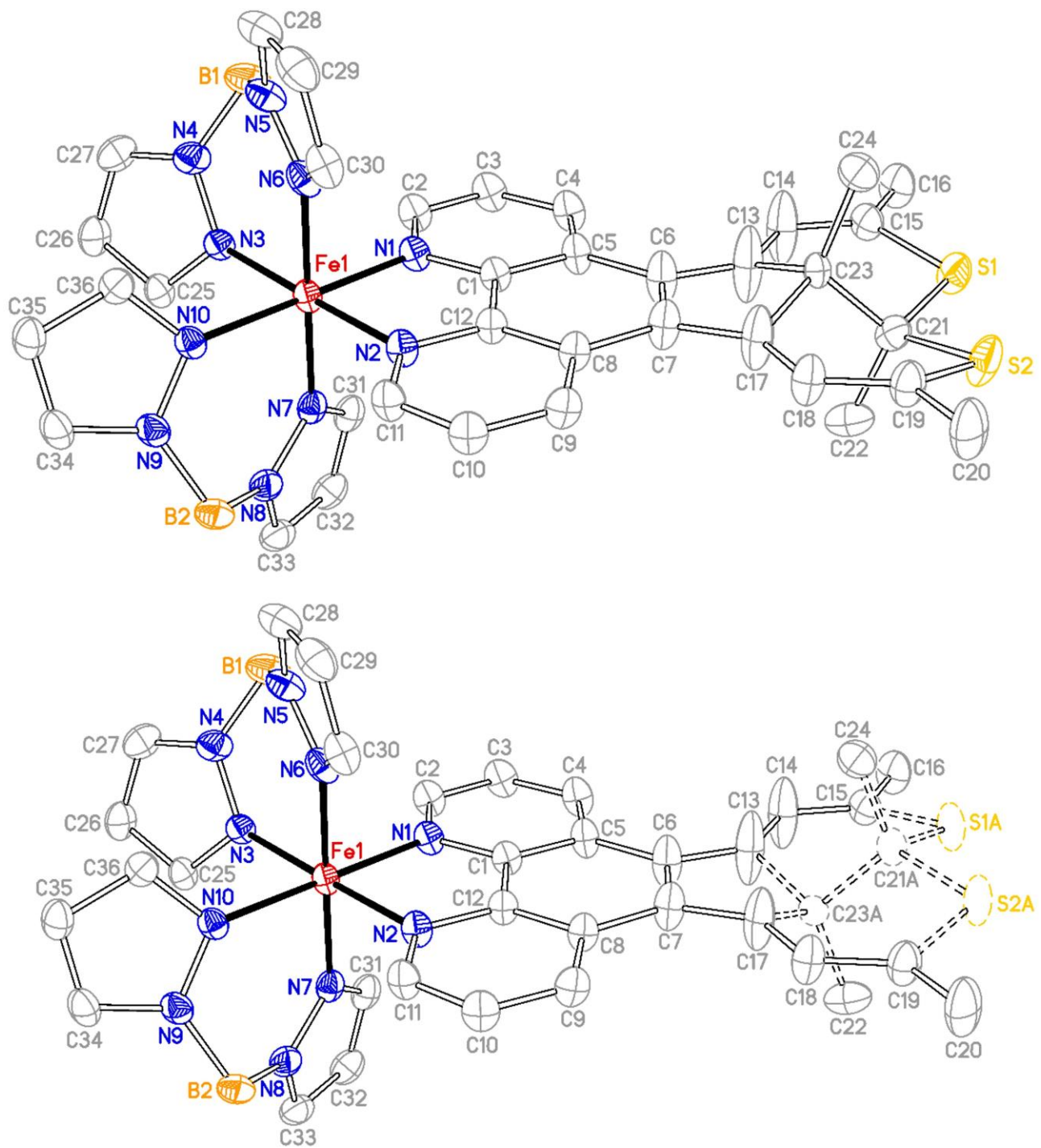


**Figure S5.** Solid-state molecular structure with the applied numbering scheme for **1-a** @ 100 K in crystals of **1-a**·(C<sub>7</sub>H<sub>8</sub>)<sub>2</sub>. Thermal ellipsoids are drawn at the 50% probability level. Hydrogen atoms and co-crystallized toluene solvent molecules are omitted for clarity. The two alternative orientations of the disordered molecule are presented (site occupancies are 51.2(6) % (top) and 48.8(6) % (bottom)).

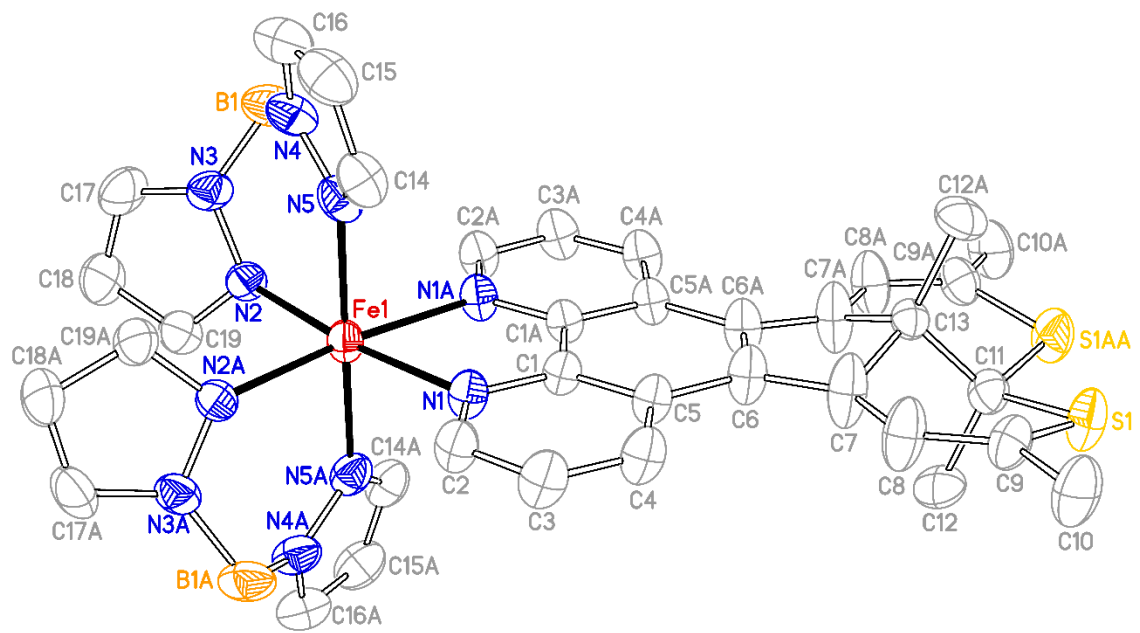


**Figure S6.** Solid-state molecular structure with the applied numbering scheme for **1-a** @ 273 K in crystals of **1-a**·(C<sub>7</sub>H<sub>8</sub>)<sub>2</sub>. Disorder, hydrogen atoms and co-crystallized toluene solvent molecules are omitted for clarity. Thermal ellipsoids are drawn at the 30% probability level.

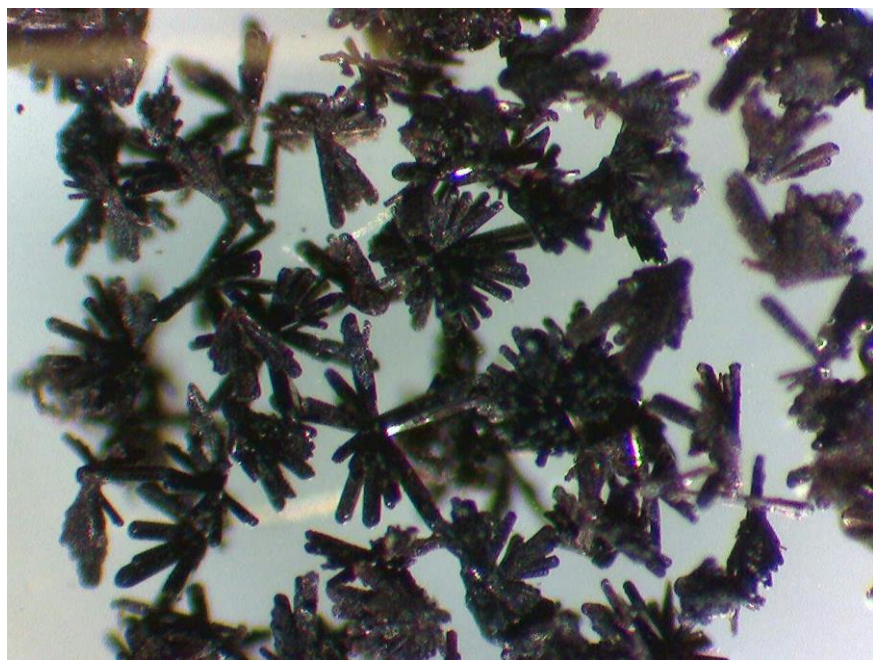


**Figure S7.** Crystals of L-a.



**Figure S8.** Crystals of 1-a.

## V. Cyclic Voltammetry

Electrochemical measurements were carried out at room temperature under nitrogen atmosphere with an Metrohm µAUTOLABIII/FRA2 potentiostat. The measurements were performed in MeCN solutions containing 0.1 M tetra-*n*-butylammonium hexafluorophosphate  $^n\text{Bu}_4\text{NPF}_6$  electrolyte, using all platinum working, counter, and pseudo-reference electrodes. Ferrocene was used as an internal standard ( $E = 0$  eV).

The first oxidation and reduction potentials  $E_p^{a1}$  and  $E_p^{c1}$  were used to determine HOMO and LUMO energy levels of **L-0** and **L-a** (see Table S9, Section IX.2), according to the equation 1<sup>13</sup> ( $e$  = elementary charge; 4.8 eV is the ionization potential of ferrocene on the vacuum scale<sup>14</sup>):

$$E_{HOMO/LUMO} = -e \cdot E_p^{a1/c1} - 4.8 \text{ eV} \quad (1)$$

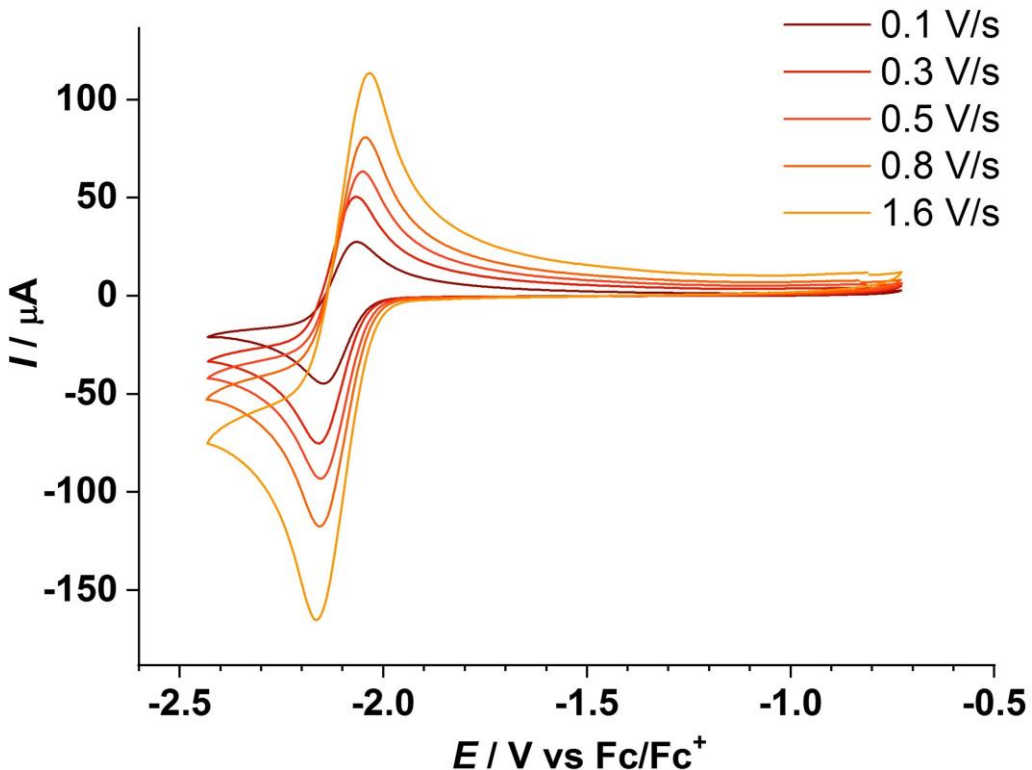


**Figure S9.** Cyclic voltammetry performed on **L-a** in acetonitrile at varying scan rates demonstrating a reversible reduction at  $V = -2.16$  V.

## VI. Magnetic Measurements

Magnetic susceptibility data for solid sample of **1-a** was collected with a Quantum Design MPMS 3 magnetometer. DC susceptibility data were collected in the temperature range 2–300 K on powder samples restrained within a polycarbonate gel capsule in the applied magnetic field of 0.1 T at 2 K min<sup>-1</sup> heating/cooling rate and 5 K intervals. The magnetic susceptibility data were corrected for underlying diamagnetism using an approximation  $\chi_m^{\text{diamag}} = \frac{1}{2} M_w \cdot 10^{-6} \text{ cm}^3 \text{ mol}^{-1}$  with  $M_w$  being the molar mass of complex.<sup>15</sup> Temperature-dependent  $\chi T$  product was fitted using the van't Hoff equation (2) to give the enthalpy and entropy changes  $\Delta H$  and  $\Delta S$ , respectively, for the LS → HS thermally-induced conversion with  $\chi_{LT}$  and  $\chi_{HT}$  being low- and high-temperature limits for molar magnetic susceptibility, respectively.

$$\chi T = \frac{\chi_{LT}T + \chi_{HT}T e^{\frac{-\Delta H + T\Delta S}{RT}}}{1 + e^{\frac{-\Delta H + T\Delta S}{RT}}} + T \cdot TIP \quad (2)$$

For Evans NMR method, a solution of **1-a** ( $c = 3.6 \cdot 10^{-4}$  M in toluene:toluene-d<sub>8</sub>:TMS = 10:2:1) was sealed in 1.5 mm capillary tube. The tube was set in 5 mm J. Young NMR tube and the same solvent mixture (toluene:toluene-d<sub>8</sub>:TMS = 10:2:1) was used as an outer standard.

Corrected temperature-dependent  $\chi_m^{\text{corr}} T$  product was obtained using equation (3).

$$\chi_m^{\text{corr}} T = \frac{3M_w \Delta f V T}{4\pi f m} - \chi_m^{\text{diamag}} T \quad (3)$$

, where  $M_w$  – molar mass of complex,  $\Delta f$  – observed frequency shift of reference resonance (Hz),  $V$  – volume of prepared solution (mL),  $T$  – working temperature (K),  $f$  – spectrometer frequency (Hz),  $m$  – mass of complex used (mg). The magnetic susceptibility data were corrected for underlying diamagnetism using the approximation  $\chi_m^{\text{diamag}} = \frac{1}{2} M_w \cdot 10^{-6} \text{ cm}^3 \text{ mol}^{-1}$ .

Temperature-dependent  $\chi T$  product was fitted using the van't Hoff equation (2) with  $\chi_{LT}$  fixed at 0. For a typical NMR spectrum, see Figure S16.

**Table S3.** Summary of parameters obtained upon fitting magnetic data (*vide supra*).

	solid state (SQUID magnetometry)		toluene solution (Evans NMR method)	
	<b>1-o</b>	<b>1-a</b>	<b>1-o</b>	<b>1-a</b>
$\chi_{HT}T,$ <sup>a</sup> cm <sup>3</sup> mol <sup>-1</sup> K	3.75(1)	3.874(6)	3.58(2)	3.78(2)
$\chi_{LT}T,$ <sup>b</sup> cm <sup>3</sup> mol <sup>-1</sup> K	0.33(1)	0.093(4)	0 (fixed)	0 (fixed)
$\Delta H,$ <sup>c</sup> kJ mol <sup>-1</sup>	11.6(3)	16.5(2)	22(2)	16.3(5)
$\Delta S,$ <sup>d</sup> J K <sup>-1</sup> mol <sup>-1</sup>	84(2)	98(1)	127(12)	84(3)
TIP, <sup>e</sup> cm <sup>3</sup> mol <sup>-1</sup>	0 (fixed)	0 (fixed)	0 (fixed)	0 (fixed)
$T_{1/2},$ <sup>f</sup> K	136.6(3)	167.7(1)	176.9(8)	195.0(3)
$T_{1/2},$ <sup>g</sup> K	137.9	165.0	-	-

<sup>a</sup> High-temperature limit of  $\chi T$  product;<sup>b</sup> Low-temperature limit of  $\chi T$  product;<sup>c</sup> Enthalpy change for LS  $\rightarrow$  HS conversion;<sup>d</sup> Entropy change for LS  $\rightarrow$  HS conversion;<sup>e</sup> Temperature independent paramagnetism;<sup>f</sup> Transition temperature determined as  $T_{1/2} = \Delta H / \Delta S$ ;<sup>g</sup> Transition temperature determined from the maximum of the first derivative  $d(\chi T)/dT$ .

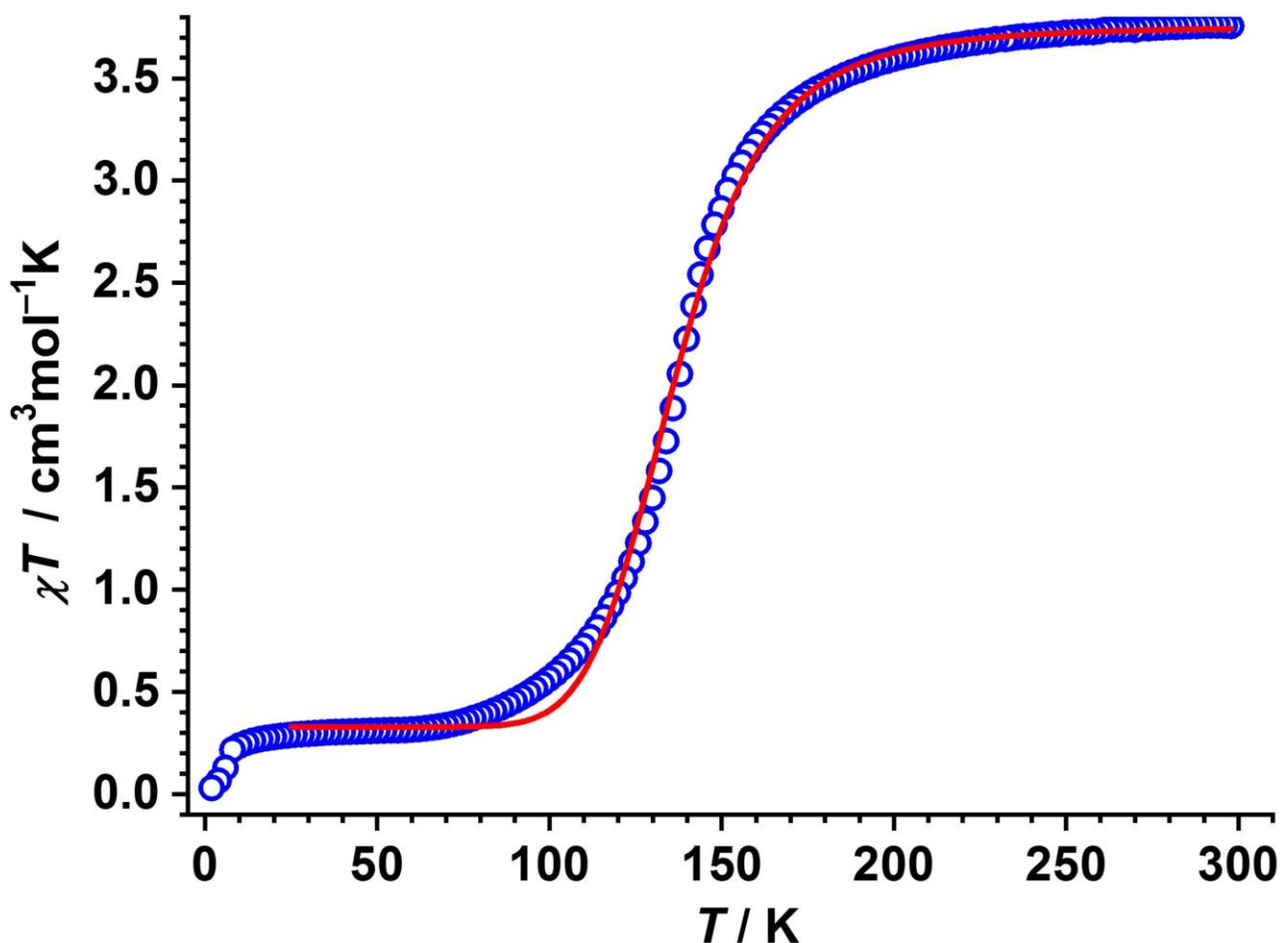


**Figure S10.** Variable temperature  $\chi T$  product of **1-o** measured on a powder sample at an external field of 1.0 T in the cooling mode (2 K intervals, 1 K min<sup>-1</sup>). Experimental data was taken from<sup>16</sup> and fitted with the van't Hoff equation (2). Fit parameters:  $\Delta H = 11.6(3)$  kJ mol<sup>-1</sup>,  $\Delta S = 84(2)$  J mol<sup>-1</sup> K,  $\chi_{LT}T = 0.33(1)$  cm<sup>3</sup> mol<sup>-1</sup> K, and  $\chi_{HT}T = 3.75(1)$  cm<sup>3</sup> mol<sup>-1</sup> K. The derived transition temperature is  $T_{1/2} = 136.6(3)$  K.

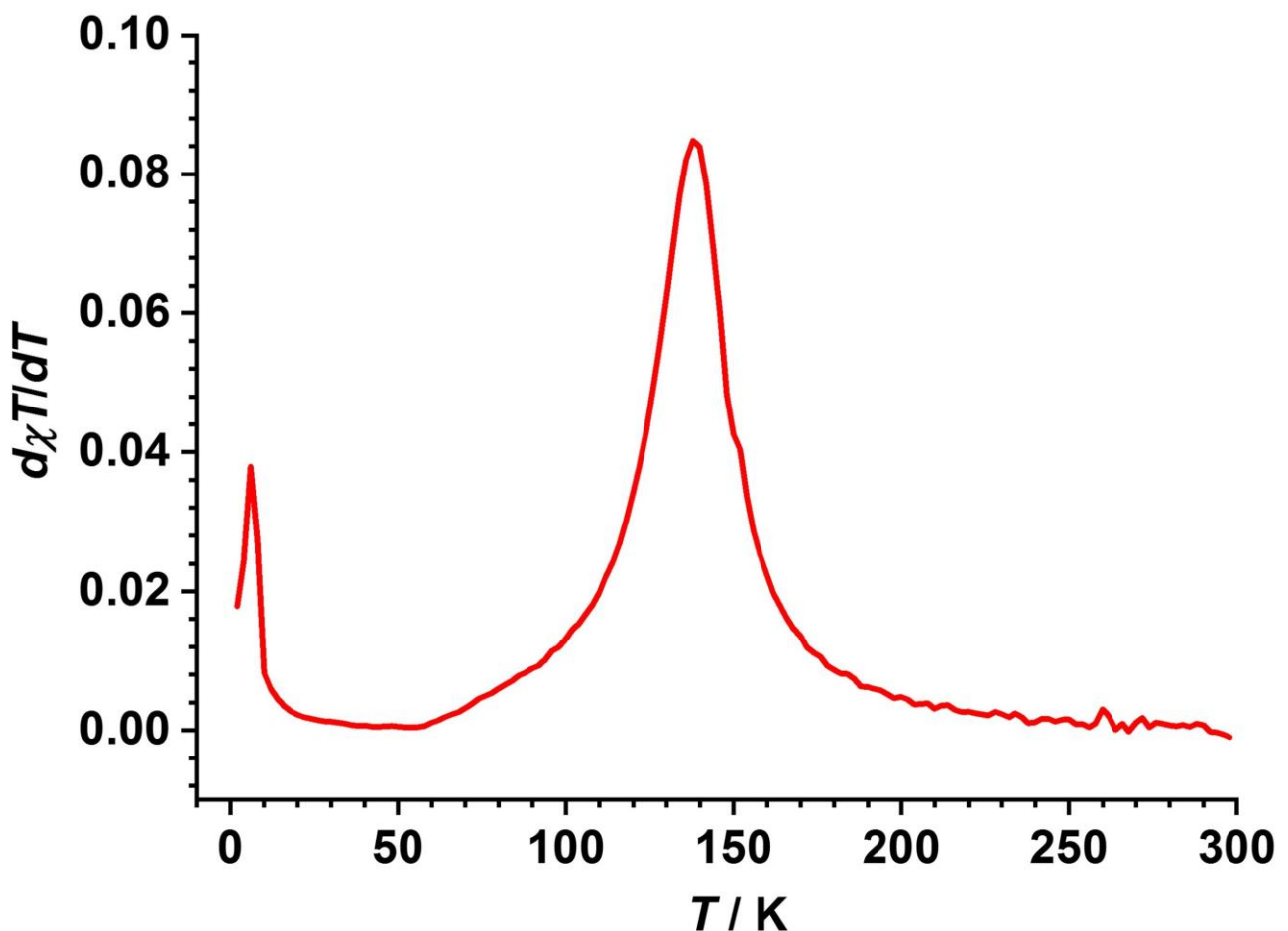


**Figure S11.** First derivative  $d(\chi T)/dT$  as a function of  $T$  for **1-o** (experimental data taken from<sup>16</sup>), showing a one-step SCO transition with a  $T_{1/2} = 137.9$  K.

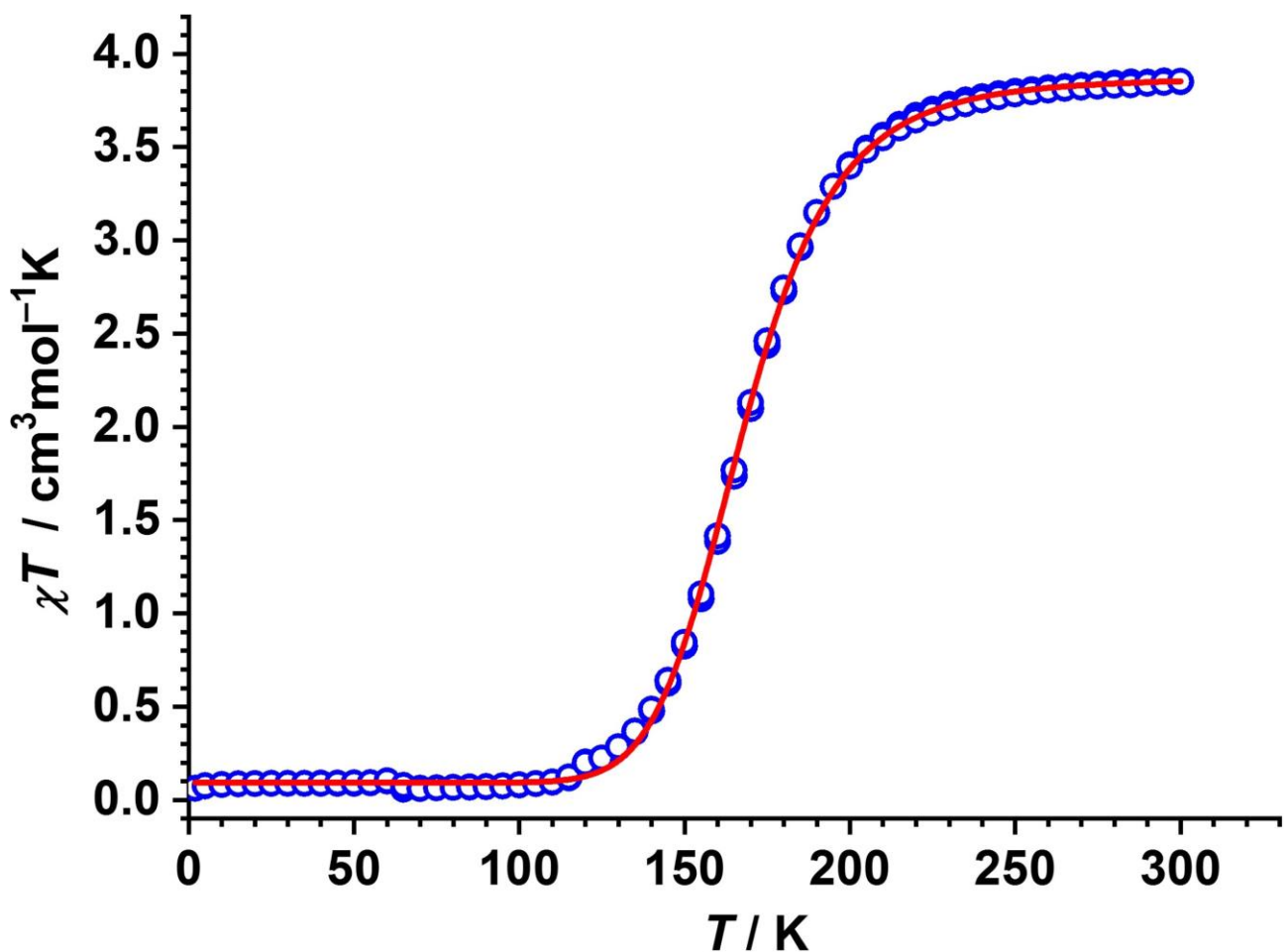


**Figure S12.** Variable temperature  $\chi T$  product of **1-a** measured on a crystalline sample at an external field of 0.1 T in the cooling mode (5 K intervals, 2 K min<sup>-1</sup>). Experimental data was fitted with the van't Hoff equation (2). Fit parameters:  $\Delta H = 16.5(2)$  kJ mol<sup>-1</sup>,  $\Delta S = 98(1)$  J mol<sup>-1</sup> K,  $\chi_{LT}T = 0.093(4)$  cm<sup>3</sup> mol<sup>-1</sup> K, and  $\chi_{HT}T = 3.874(6)$  cm<sup>3</sup> mol<sup>-1</sup> K. The derived transition temperature is  $T_{1/2} = 167.7(1)$  K.

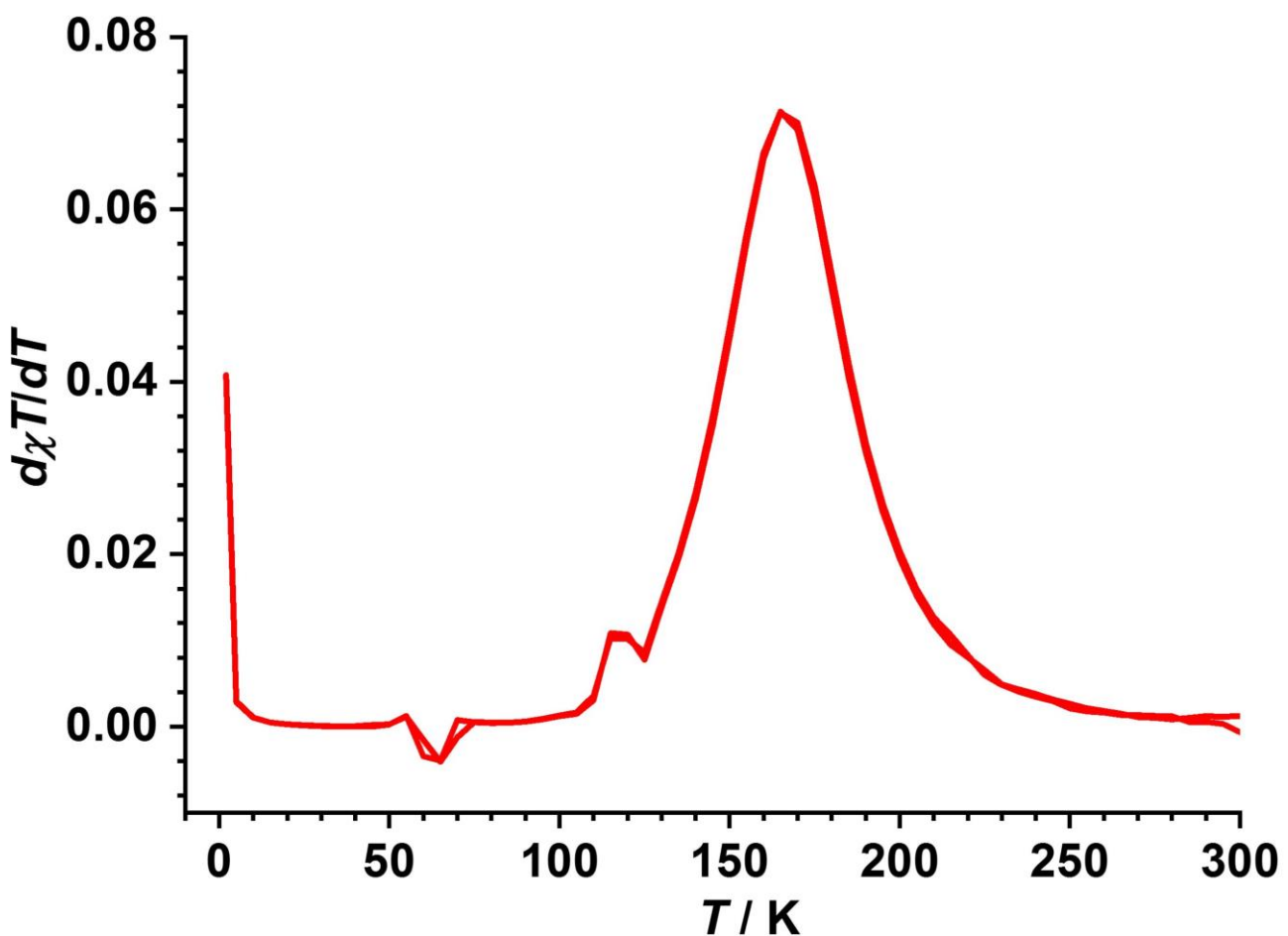


**Figure S13.** First derivative  $d(\chi T)/dT$  as a function of  $T$  for **1-a**, showing a one-step SCO transition with a  $T_{1/2} = 165.0$  K.

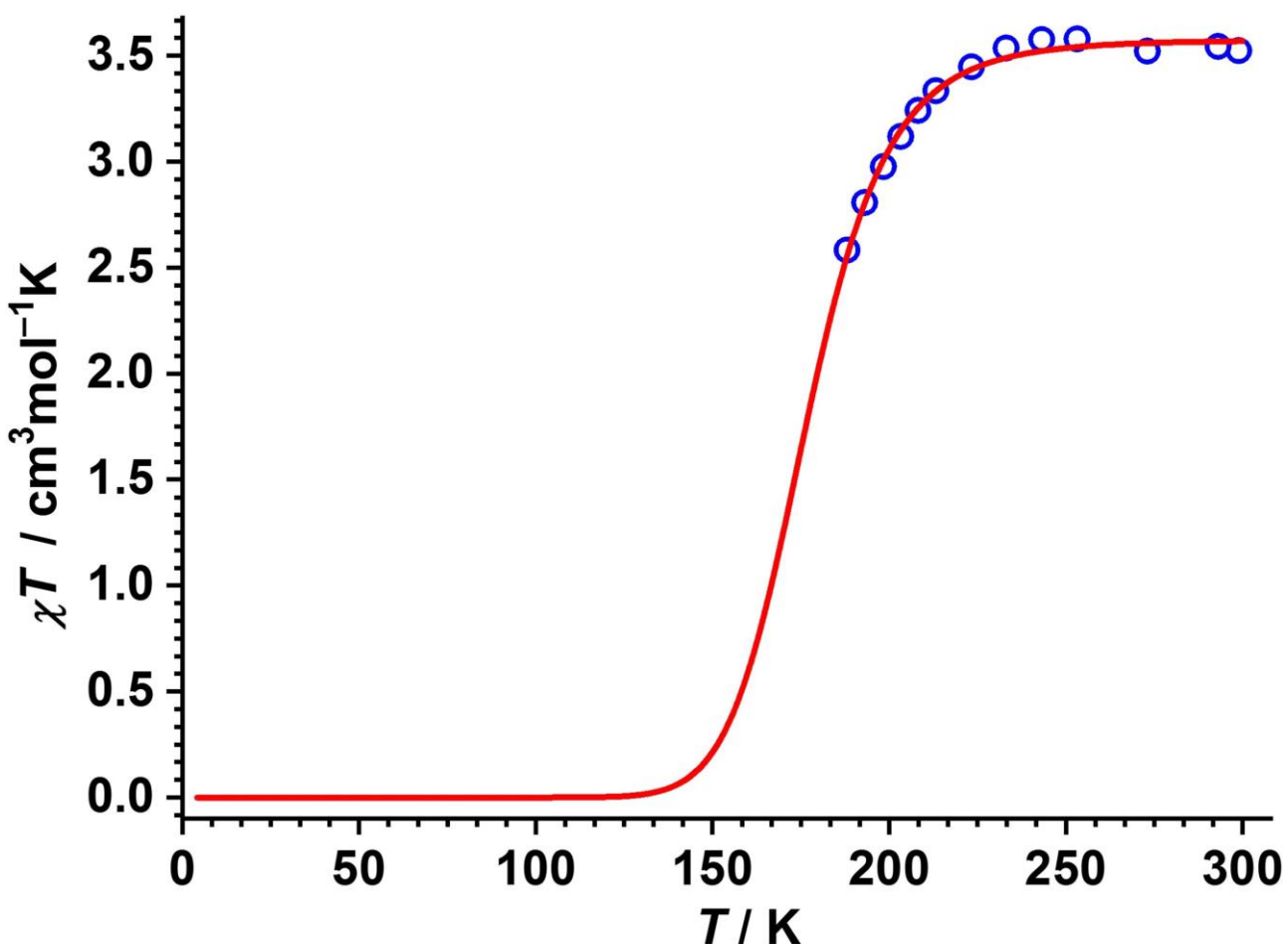


**Figure S14.** Temperature dependent  $\chi T$  product of **1-o** measured with the Evans NMR method in toluene:toluene- $d_8$ :TMS = 10:2:1 solution. TMS signal was used for analysis. Experimental data was taken from<sup>16</sup> and fitted with the van't Hoff equation (2). Fit parameters:  $\Delta H = 22(2)$  kJ mol<sup>-1</sup>,  $\Delta S = 127(12)$  J K<sup>-1</sup> mol<sup>-1</sup>,  $\chi_{LT}T = 0$  (fixed), and  $\chi_{HT}T = 3.58(2)$  cm<sup>3</sup> mol<sup>-1</sup> K. The derived transition temperature is  $T_{1/2} = 176.9(8)$  K.

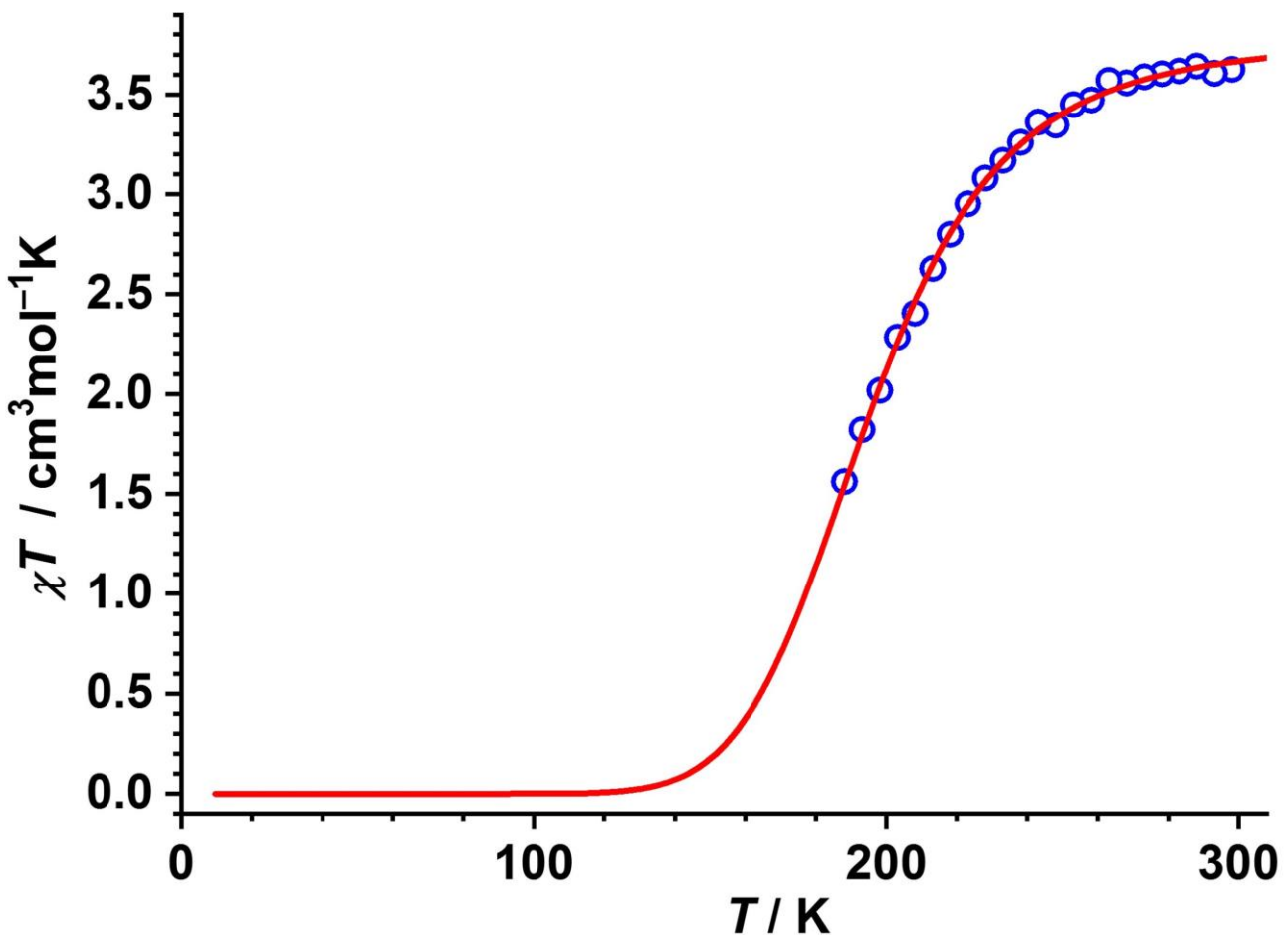


**Figure S15.** Temperature dependent  $\chi T$  product of **1-a** measured with the Evans NMR method in toluene:toluene-*d*<sub>8</sub>:TMS = 10:2:1 solution. TMS signal was used for analysis. Fitting parameters:  $\Delta H = 16.3(5)$  kJ mol<sup>-1</sup>,  $\Delta S = 84(3)$  J K<sup>-1</sup> mol<sup>-1</sup>,  $\chi_{LT}T = 0$  (fixed), and  $\chi_{HT}T = 3.78(2)$  cm<sup>3</sup> mol<sup>-1</sup> K. The derived transition temperature is  $T_{1/2} = 195.0(3)$  K.

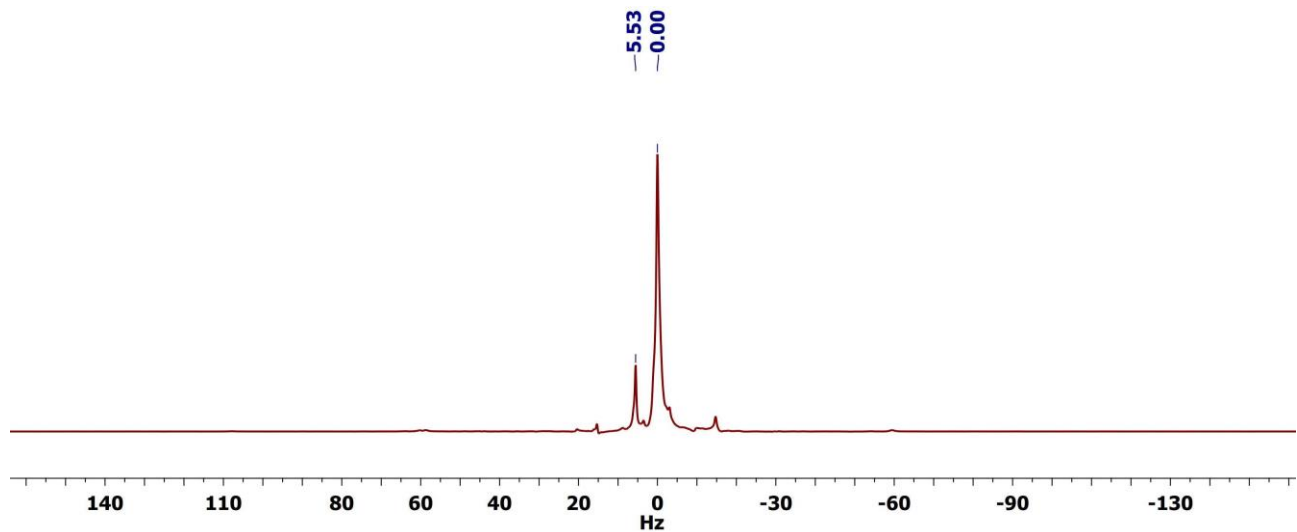


**Figure S16.** Evans measurements: exemplary  $^1\text{H}$  NMR spectrum of **1-a** ( $c = 3.6 \cdot 10^{-4}$  M in toluene:toluene-d<sub>8</sub>:TMS = 10:2:1,  $T = 233$  K, inside a capillary) with an outside reference (toluene:toluene-d<sub>8</sub>:TMS = 10:2:1).

## VII. Mössbauer Spectroscopy

Mössbauer spectra were recorded on a conventional spectrometer with alternating constant acceleration of the  $\gamma$  - source ( $^{57}\text{Co}/\text{Rh}$ , 1.8 GBq). The raw data sets (512 channels) were folded to merge the recorded two linear mirror images of the spectra which also eliminates the parabolic background. The minimum experimental line width was  $0.24 \text{ mms}^{-1}$  (full width at half-height). Isomer shifts are quoted relative to iron metal at 300 K as the spectrometer was calibrated by recording the Mössbauer spectrum of a  $12 \mu\text{m}$  thick foil of  $\alpha$ -Fe at room temperature, with the center of the six-line pattern being taken as zero velocity. The sample temperature was maintained constant in an Oxford Instruments Variox cryostat. mf.SL package (Eckhard Bill, version 2.2) was used to simulate the spectra with Lorentzian doublets, or doublet Voigt profiles, with least-squares parameter optimization.<sup>17</sup>

**Table S4.** Fit parameters for zero-field  $^{57}\text{Fe}$  Mössbauer spectra collected on a crystalline sample of **1-a** at different temperatures.

		80 K			160 K			260 K		
		$\delta$ , mm $\text{s}^{-1}$	$ \Delta E_Q $ , mm $\text{s}^{-1}$	rel. int., %	$\delta$ , mm $\text{s}^{-1}$	$ \Delta E_Q $ , mm $\text{s}^{-1}$	rel. int., %	$\delta$ , mm $\text{s}^{-1}$	$ \Delta E_Q $ , mm $\text{s}^{-1}$	rel. int., %
<b>LS</b>	component 1	0.51	0.52	48	0.56	0.66	62	-	-	-
	component 2	0.52	0.96	52				-	-	-
<b>HS</b>	component 1	-	-	-	1.03	1.84	38	1.02	1.39	45
	component 2	-	-	-				1.09	1.56	55

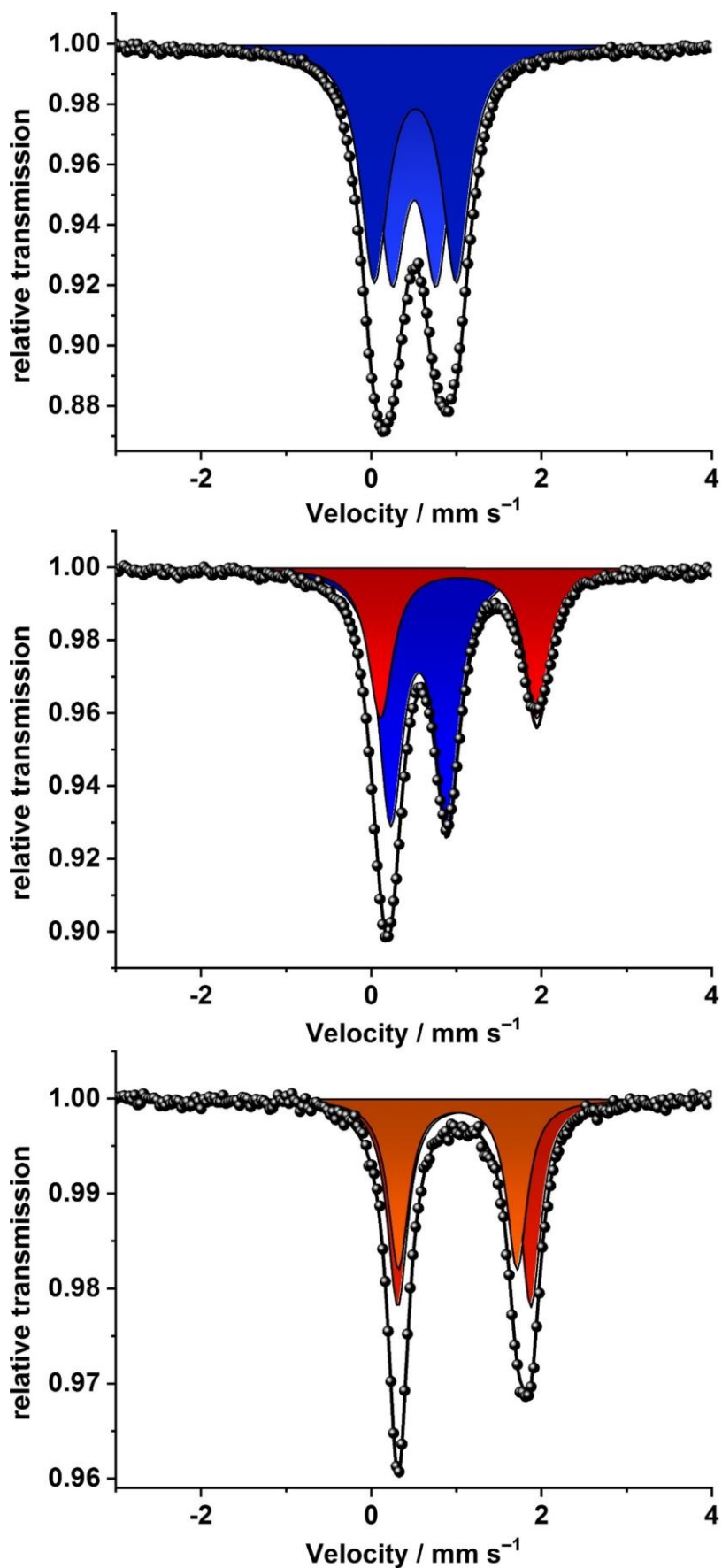


**Figure S17.** Zero-field  $^{57}\text{Fe}$  Mössbauer spectra measured on a crystalline sample of **1-a** at 80 (top), 160 (middle), and 260 K (bottom). For details, see Table S4.

## VIII. Photochemistry

Electronic absorption spectra were recorded with a Shimadzu UV 3600 spectrophotometer.

All solutions for photoexperiments were prepared and sealed under inert conditions.

Absorption spectra were measured in custom made Quartz SUPRASIL (QS) 1 cm cells. NMR studies were performed in J. Young quartz tube. Irradiation was performed by one or four UV analytical lamps (Herolab,  $\lambda = 313$  and  $365$  nm,  $15$  W each). Preparative photoreactions were conducted in a  $250$  mL quartz flask positioned between four opposing UV analytical lamps (Herolab,  $\lambda = 313$  and  $365$  nm,  $15$  W each).

The quantum yields of photocyclization and cycloreversion ( $\Phi_{AB}$  and  $\Phi_{BA}$ ) were measured by previously reported method in air-saturated solutions.<sup>18</sup> 1,2-Bis(2-methyl-1-benzothiophen-3-yl)perfluorocyclopentene in *n*-hexane solution was used as a chemical actinometer at  $313$  and  $520$  nm.<sup>18</sup> An LOT-Oriel Xe-OFR arc lamp ( $1\text{kW}$ ) equipped with an Omni- $\lambda$  300 monochromator was used as a wavelength-variable light source. The measured photon numbers per second were  $1.7 \times 10^{15}$  photons/sec for  $313$  nm and  $9.2 \times 10^{15}$  photons/sec for  $520$  nm.

Molar extinction coefficient of the photogenerated isomer **L-c** was determined by  $^1\text{H}$  NMR and UV/Vis spectroscopy ( $l = 0.1$  cm, quartz cuvette) of pre-irradiated solution of **L-o**. Five *independent* samples were studied before plotting them by equation 4.

$$\varepsilon_c = \frac{A}{conv \cdot c_0 \cdot l} \quad (4)$$

, where  $A$  is the absorption at band maximum of the photogenerated isomer at  $510$  nm;  $conv$  is the conversion of **L-o**;  $c_0$  is the total concentration of the compound. The molar extinction coefficient of **L-c** was found to be  $5000 \text{ M}^{-1}\text{cm}^{-1}$  at  $510$  nm.

### VIII.1. NMR studies

**Scheme S1.** Photochemical reactions of **L-o**.

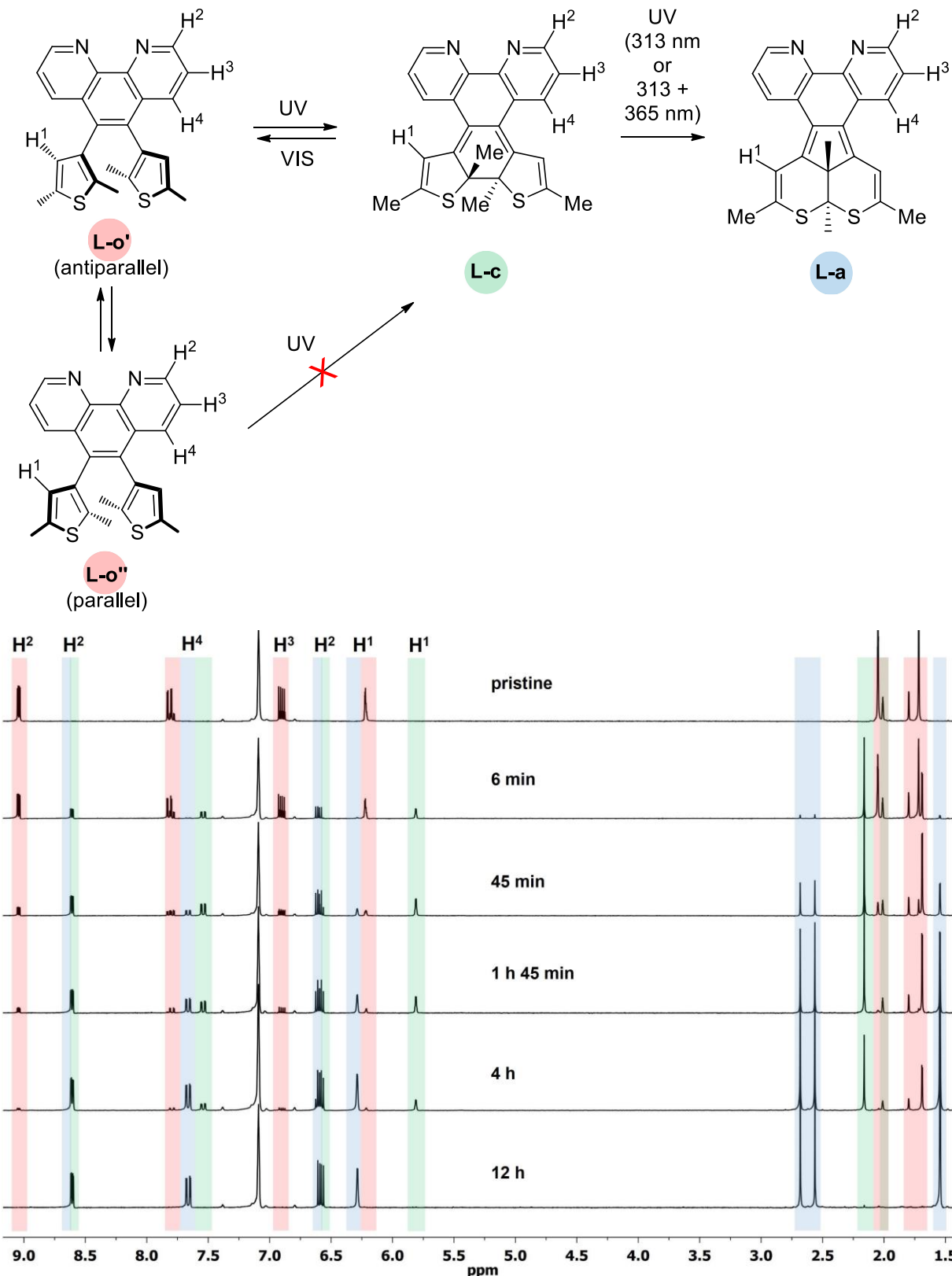


**Figure S18.** <sup>1</sup>H NMR spectra (270 MHz) of **L-o** ( $5.0 \times 10^{-3}$  M, oxygen-free C<sub>6</sub>D<sub>6</sub>) upon UV irradiation ( $\lambda = 313$  nm, 4 × 16W) (full version of Figure 2).

**Table S5.** Assignment of  $^1\text{H}$  NMR signals (ppm) for **L-o**, **L-c**, and **L-a** (270 MHz,  $5.0 \times 10^{-3}$  M,  $\text{C}_6\text{D}_6$ ).

	<b>L-o*</b>	<b>L-c</b>	<b>L-a</b>
$\text{H}^1$	6.22 (m) <sup>†</sup>	5.81 (s)	6.29 (d, $J = 1.1$ Hz)
$\text{H}^2$	9.04 (dd, $J = 4.2, 1.8$ Hz)**	8.61 (dd, $J = 4.4, 1.7$ Hz) <sup>‡</sup>	8.61 (dd, $J = 4.4, 1.7$ Hz) <sup>‡</sup>
$\text{H}^3$	major: 6.90 (dd, $J = 8.3, 4.2$ Hz) minor: 6.90 (dd, $J = 8.3, 4.2$ Hz)	6.60 (dd, $J = 8.1, 4.4$ Hz)	6.59 (dd, $J = 8.2, 4.4$ Hz)
$\text{H}^4$	major: 7.82 (dd, $J = 8.3, 1.8$ Hz) minor: 7.79 (dd, $J = 8.3, 1.8$ Hz)	7.54 (dd, $J = 8.1, 1.7$ Hz)	7.66 (dd, $J = 8.2, 1.7$ Hz)
Me	major: 1.72 (s), 2.05 (s) minor: 1.80 (s), 2.01 (s)	2.16 (s), 2.72 (s)	1.54 (d, $J = 1.1$ Hz) 2.56 (s), 2.68 (s)

\* Both antiparallel **L-o'** and parallel **L-o''** conformers

† Two sets of signals for the parallel and antiparallel conformations were not well-resolved

‡ Two sets of signals for the **L-c** and **L-a** were not well-resolved

After 7 h of irradiation of a **L-o** solution at  $\lambda = 313$  nm only, the reaction mixture contained 93% of **L-a**, 3% of **L-o**, and 4% of the intermediate **L-c** (Figure S19). After irradiation of a similar solution for 7 h at  $\lambda = 313$  and 365 nm simultaneously, the reaction mixture contained 98% of **L-a** and 2% of **L-c** (Figure S20). Thus, a simultaneous usage of two light sources (313 and 365 nm) resulted in a slightly increased yield of **L-a** isomer.

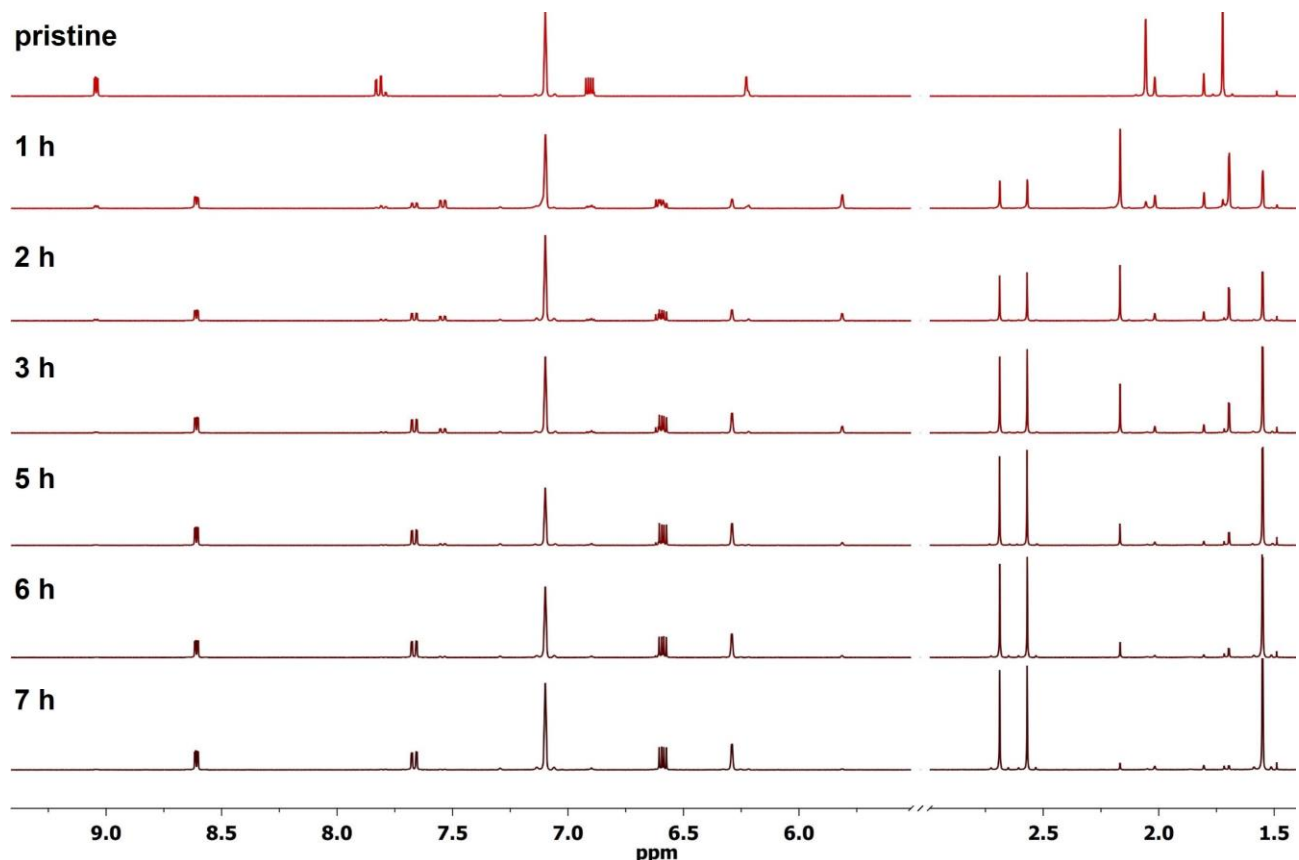


**Figure S19.**  $^1\text{H}$  NMR spectra of **L-o** ( $2.1 \times 10^{-3}$  M, degassed benzene- $d_6$ ) upon UV irradiation at  $\lambda = 313$  nm (4  $\times$  16W).

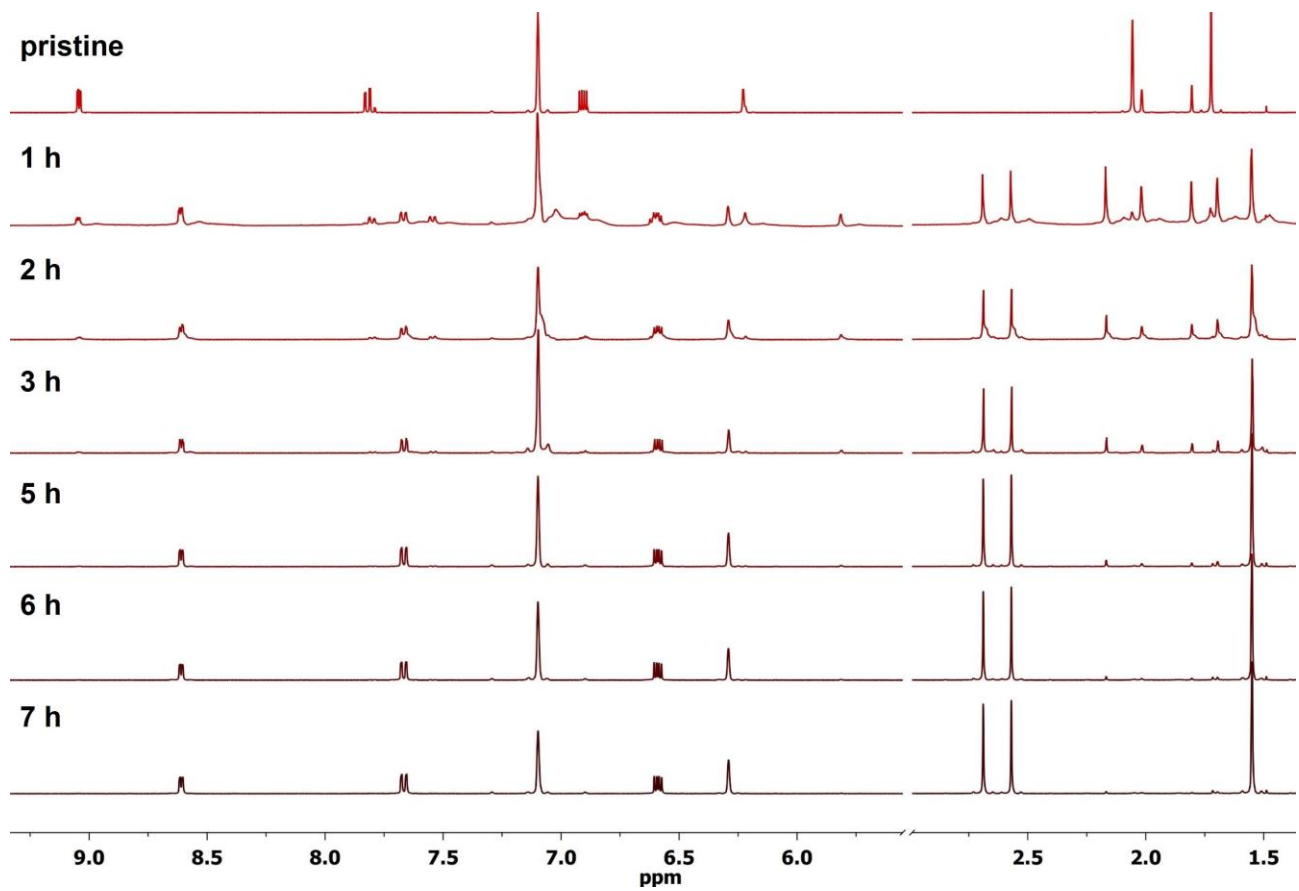


**Figure S20.** <sup>1</sup>H NMR spectra of **L-o** ( $2.1 \times 10^{-3}$  M, degassed benzene-*d*<sub>6</sub>) upon UV simultaneous irradiation at  $\lambda = 313$  nm (4 × 16W) and  $\lambda = 365$  nm (4 × 16W).

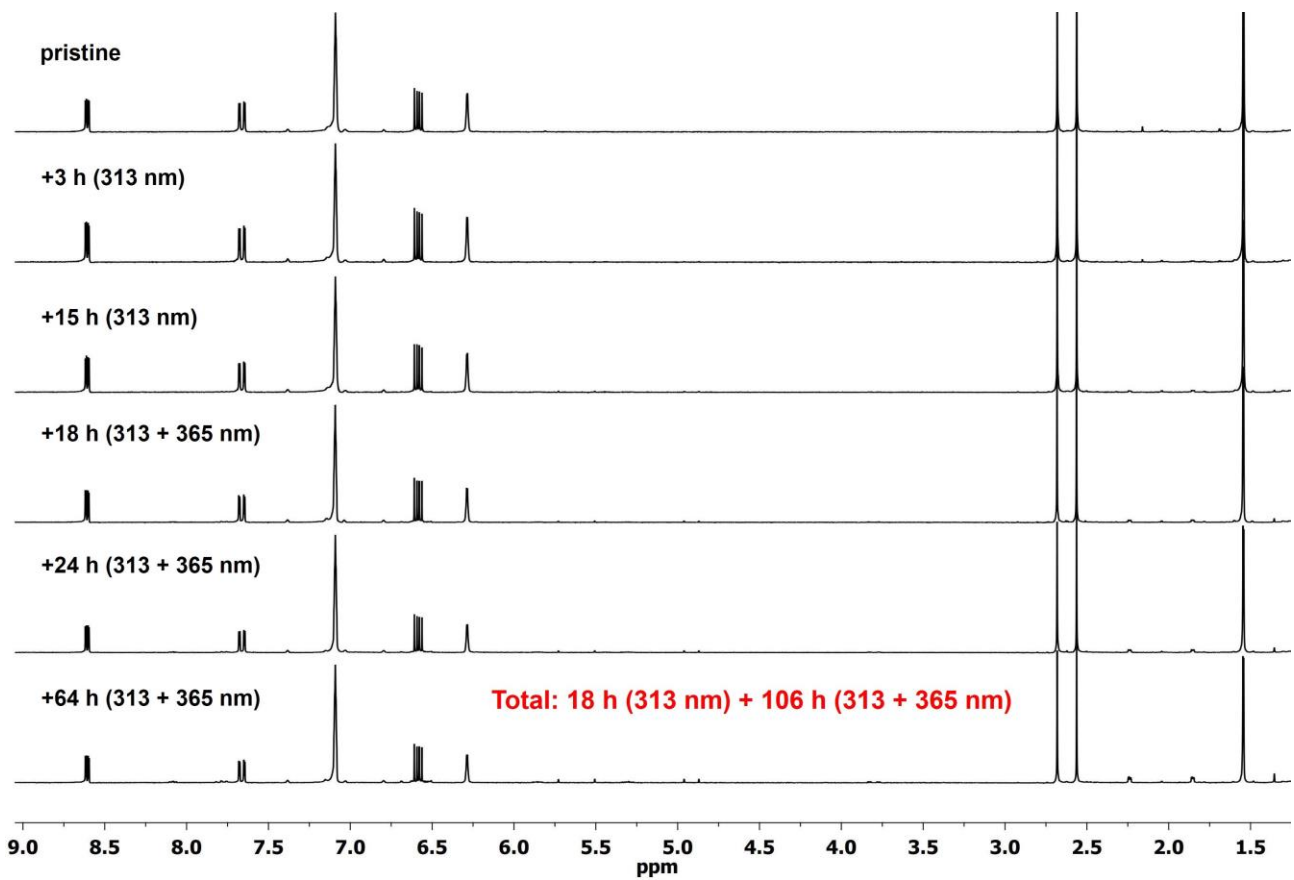


**Figure S21.** Photostability of **L-a**: <sup>1</sup>H NMR spectra (270 MHz) of **L-a** solution upon continuous UV irradiation ( $\lambda = 313$  or  $313+365$  nm,  $4 \times 16\text{W}$ ).

### VIII.2. Electronic absorption spectroscopy

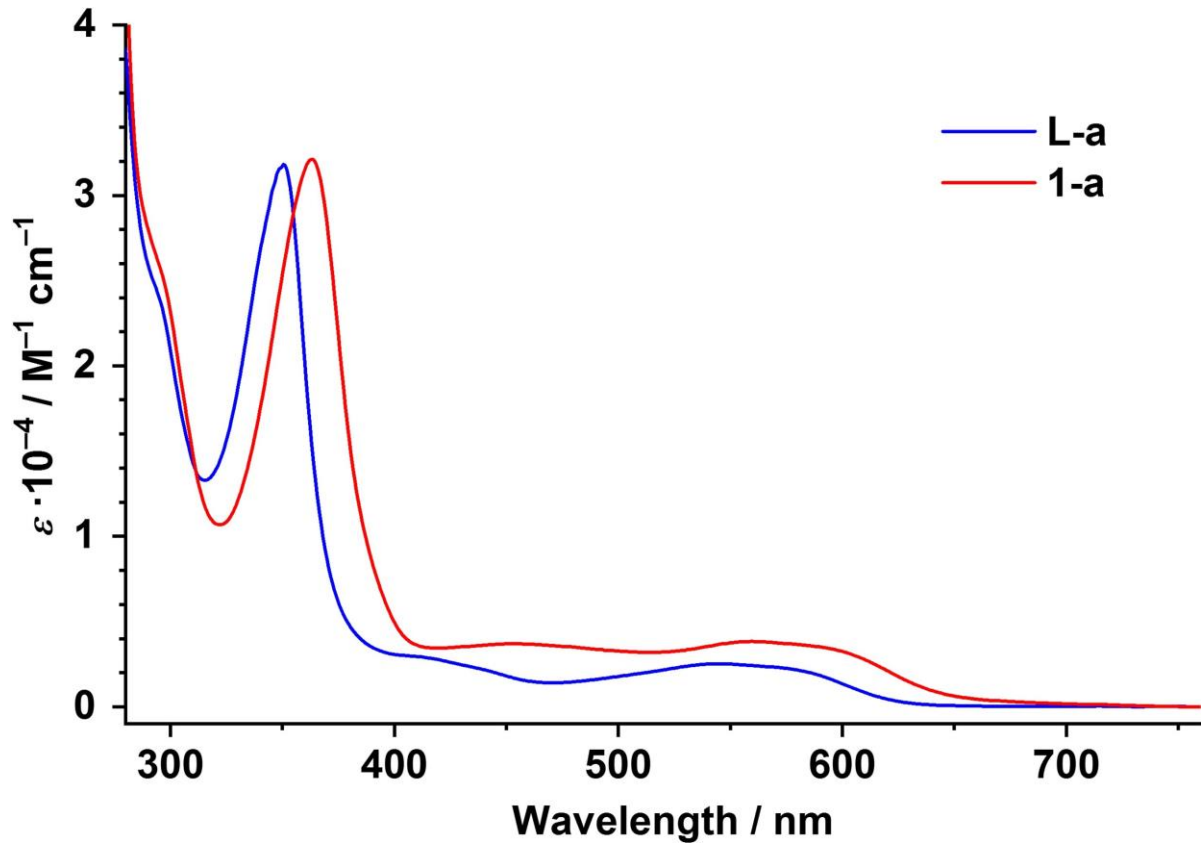


**Figure S22.** Absorption spectra of **L-a** and **1-a** in toluene.

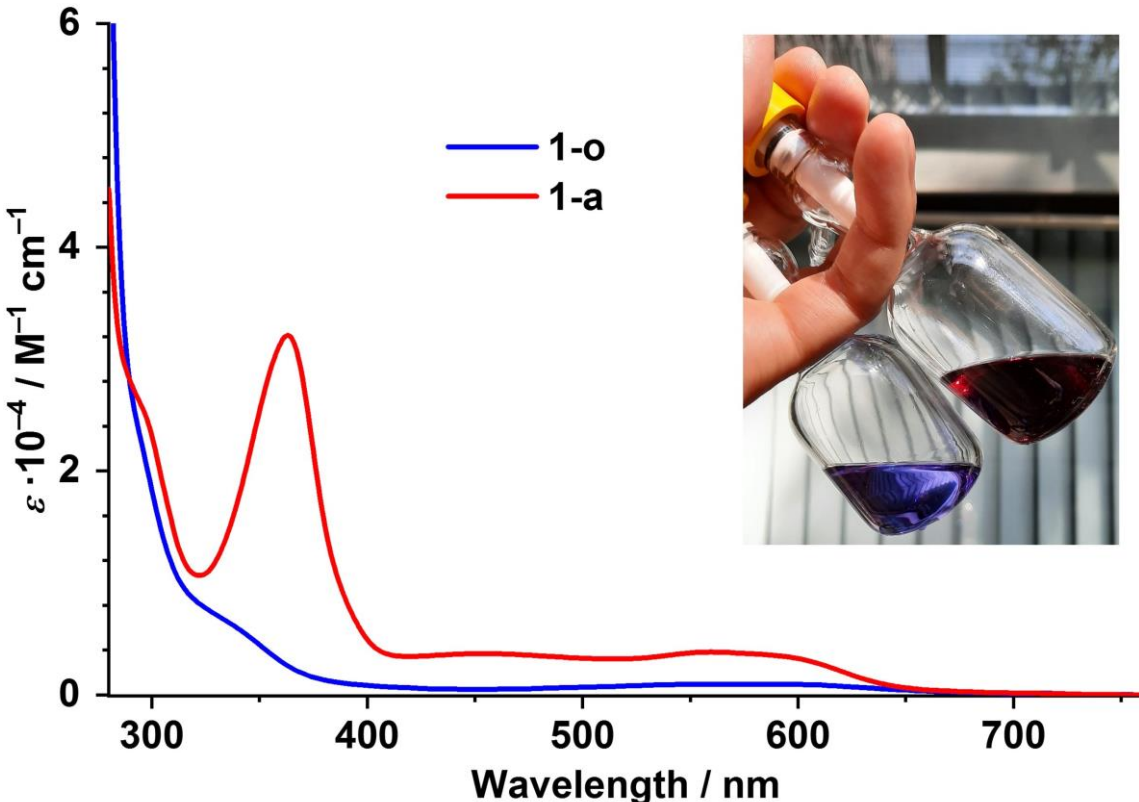


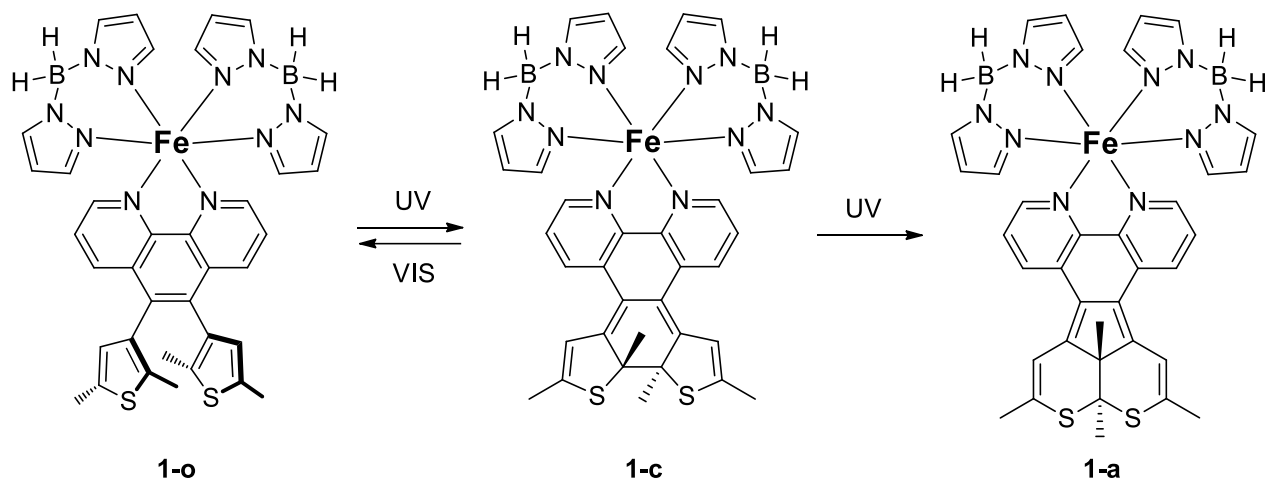
**Figure S23.** Absorption spectra of complexes **1-o** (blue solution on the inset) and **1-a** (red solution on the inset) in toluene.

**Table S6.** Absorption maxima and molar extinction coefficients of **L-a** and **1-a** in toluene.

	<b>L-a</b>	<b>1-a</b>
$\lambda$ , nm ( $\epsilon$ , M <sup>-1</sup> cm <sup>-1</sup> )	351 (31800) 411 (2900) <sup>sh*</sup> 545 (2500) 572 (2300) <sup>sh</sup>	364 (32100) 454 (3700) <sup>sh</sup> 560 (3800) 590 (3500) <sup>sh</sup>

\* Shoulder

**Scheme S2.** Photochemical reactions of complex **1-o**.



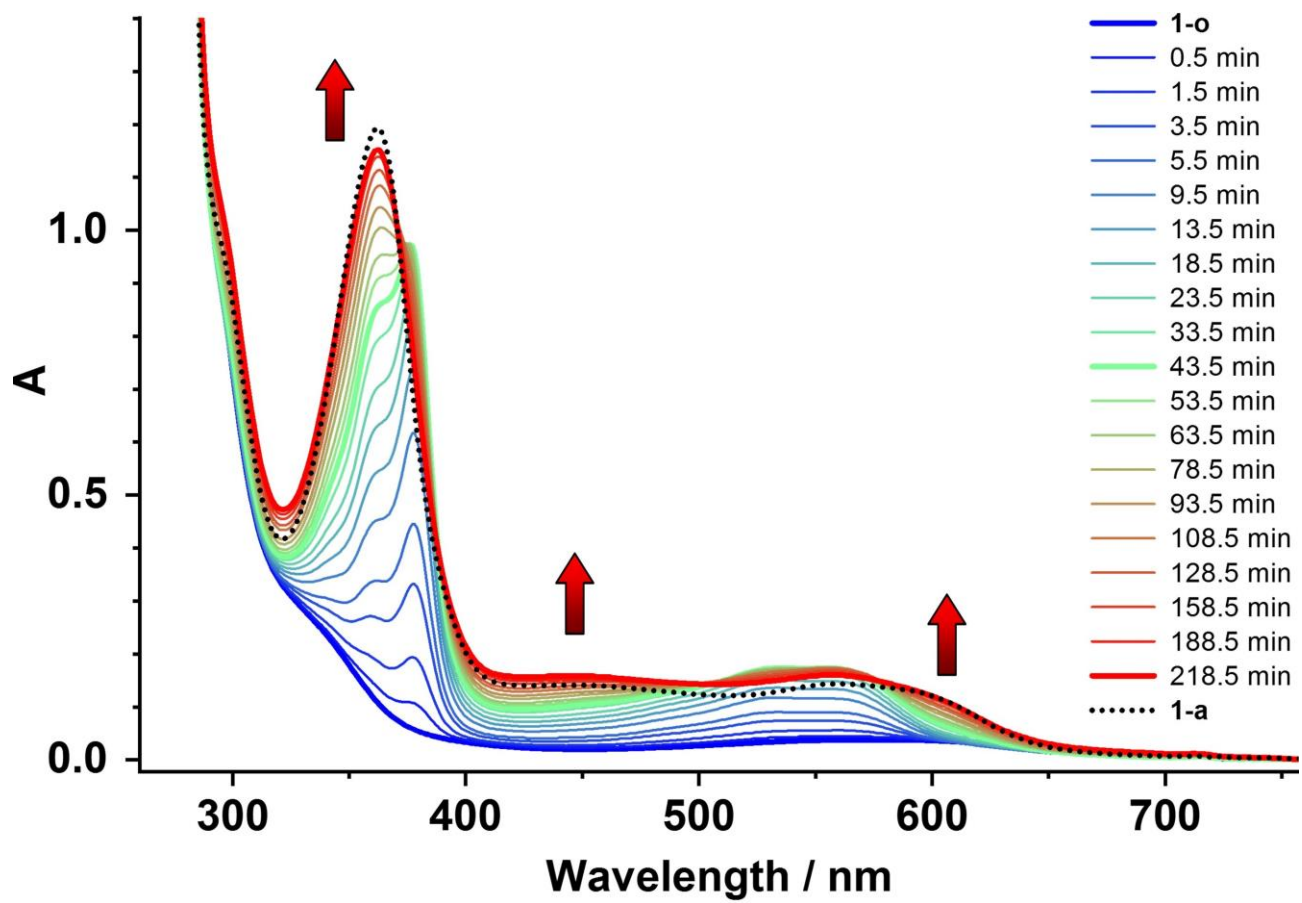


**Figure S24.** Evolution of absorption bands of complex **1-o** in toluene ( $c = 4 \cdot 10^{-5}$  M) upon UV irradiation ( $\lambda = 313$  nm, 16W), showing initial photocyclization to **1-c** (pseudo-PSS) and subsequent isomerization to **1-a**. Figure S25 and Figure S26 show the processes separately.

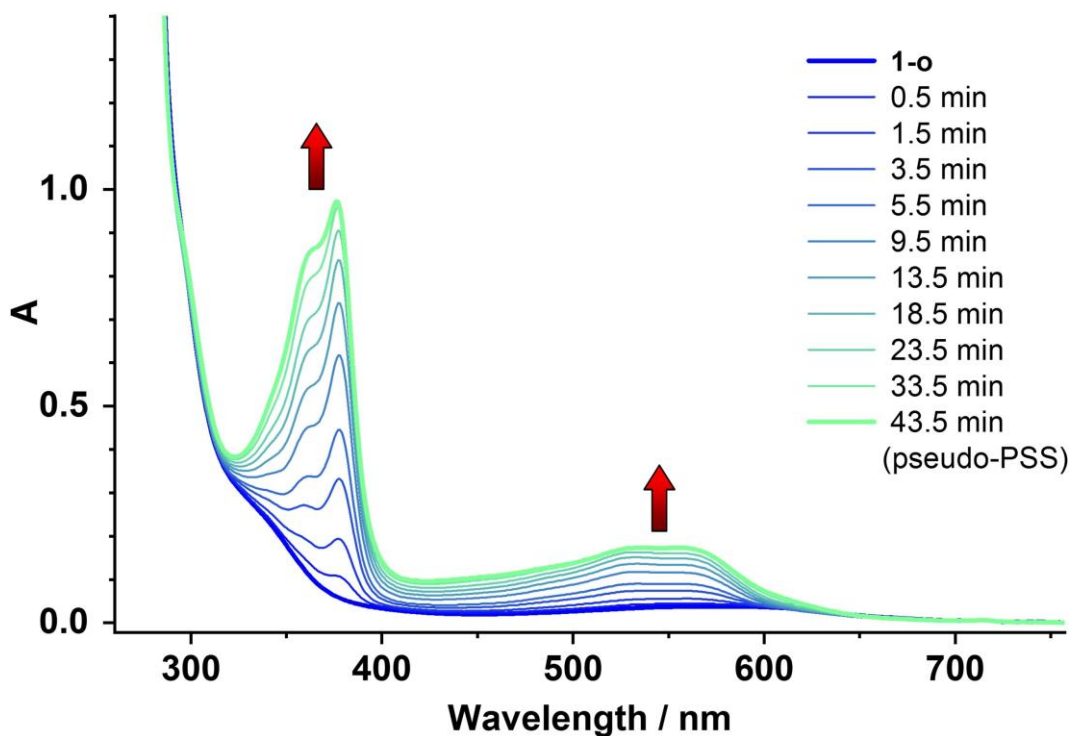


**Figure S25.** Evolution of absorption bands of complex **1-o** in toluene ( $c = 4 \cdot 10^{-5}$  M) upon UV irradiation ( $\lambda = 313$  nm, 16W) from pristine to 43.5 min (pseudo-PSS), revealing a **1-o**  $\rightarrow$  **1-c** photocyclization.

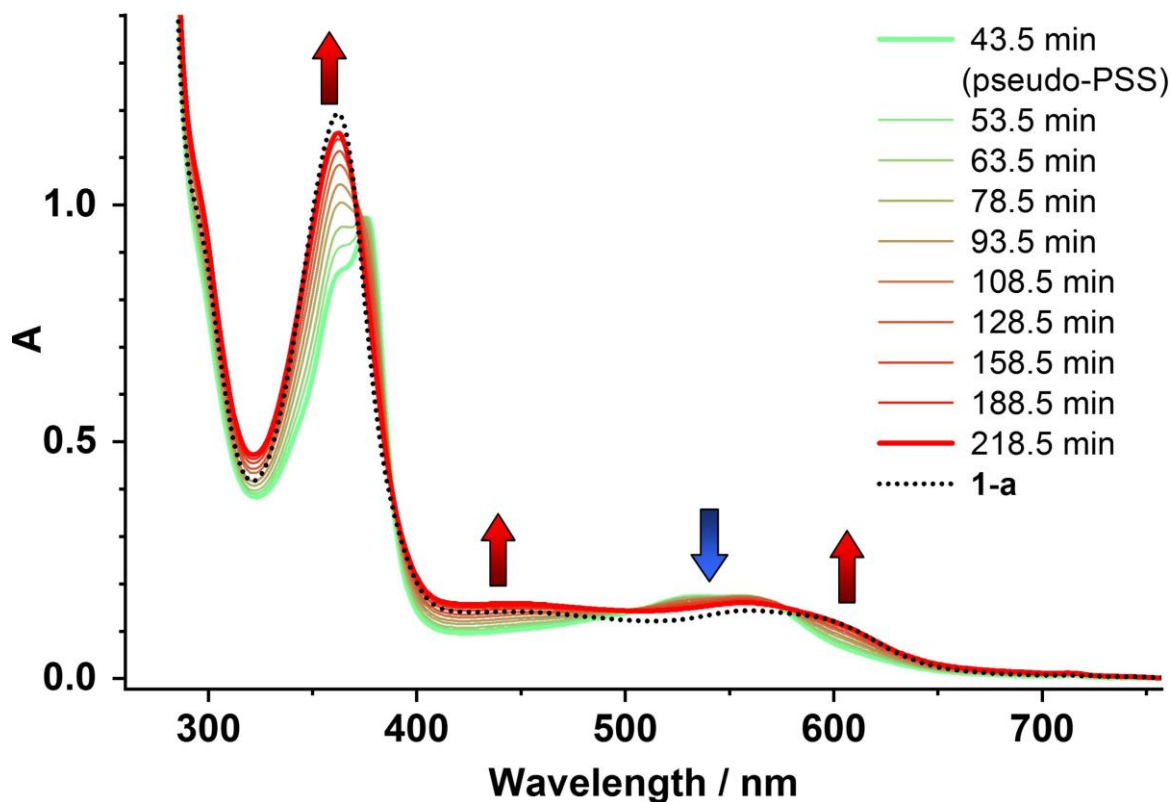


**Figure S26.** Continued evolution of absorption bands of **1-o** in toluene ( $c = 4 \cdot 10^{-5}$  M) upon UV irradiation ( $\lambda = 313$  nm, 16W) from 43.5min (pseudo-PSS) to 218.5 min, revealing predominantly a **1-c**  $\rightarrow$  **1-a** isomerization.

## IX. DFT Calculations

General. Density functional theory (DFT) calculations were performed using the Gaussian 09 program package.<sup>19</sup> Calculations of vibrational frequencies were performed to prove that each optimized structure corresponds to a true minimum on the potential energy surface. The solvent influence was modeled using the polarizable continuum model (PCM)<sup>20</sup> with acetonitrile or toluene.

Optimization of L-o and L-a. Ground state geometry optimizations were performed using PBE0,<sup>21</sup> BVP86,<sup>22</sup> and B3LYP<sup>23</sup> functionals with 6-311+G(d,p), 6-31G(d,p), and 6-31G(d) basis sets, respectively, in gas phase or in acetonitrile (PCM).

Calculations of electronic absorption spectra of L-c and L-a were performed according to Masunov *et al.*<sup>24</sup> Geometry optimization was performed using the M05-2x<sup>25</sup> functional with the 6-31G(d) basis set in toluene (PCM). The absorption spectra were calculated by linear-response time-dependent DFT (TD-DFT)<sup>26</sup> using M05<sup>27</sup> functional with the 6-31G(d) basis set in toluene (PCM). Calculated spectra were generated by employing Gaussian-shaped absorption bands with 1500 cm<sup>-1</sup> (Half-Width at Half Height).

### IX.1. Calculated electronic absorption spectra for L-c and L-a

**Table S7.** Calculated wavelength  $\lambda$  (nm) and oscillator strength  $f$  for **L-c** (M05-2x/6-31G(d)/PCM(toluenе)//TD-M05/6-31G(d)/PCM(toluenе) level of theory).

Excited state	$\lambda$ , nm	$f$
1	542	0.1277
2	402	0.0226
3	380	0.1323
4	353	0.4766
5	323	0.0248
6	321	0.0463
7	317	0.0136
8	301	0.0216
9	300	0.0525
10	294	0.0033

**Table S8.** Calculated wavelength  $\lambda$  (nm) and oscillator strength  $f$  for **L-a** (M05-2x/6-31G(d)/PCM(toluenе)//TD-M05/6-31G(d)/PCM(toluenе) level of theory).

Excited state	$\lambda$ , nm	$f$
1	580	0.0608
2	409	0.0247
3	374	0.1139
4	351	0.6714
5	331	0.0057
6	312	0.0105
7	301	0.0121
8	300	0.0311
9	299	0.0375
10	289	0.0169

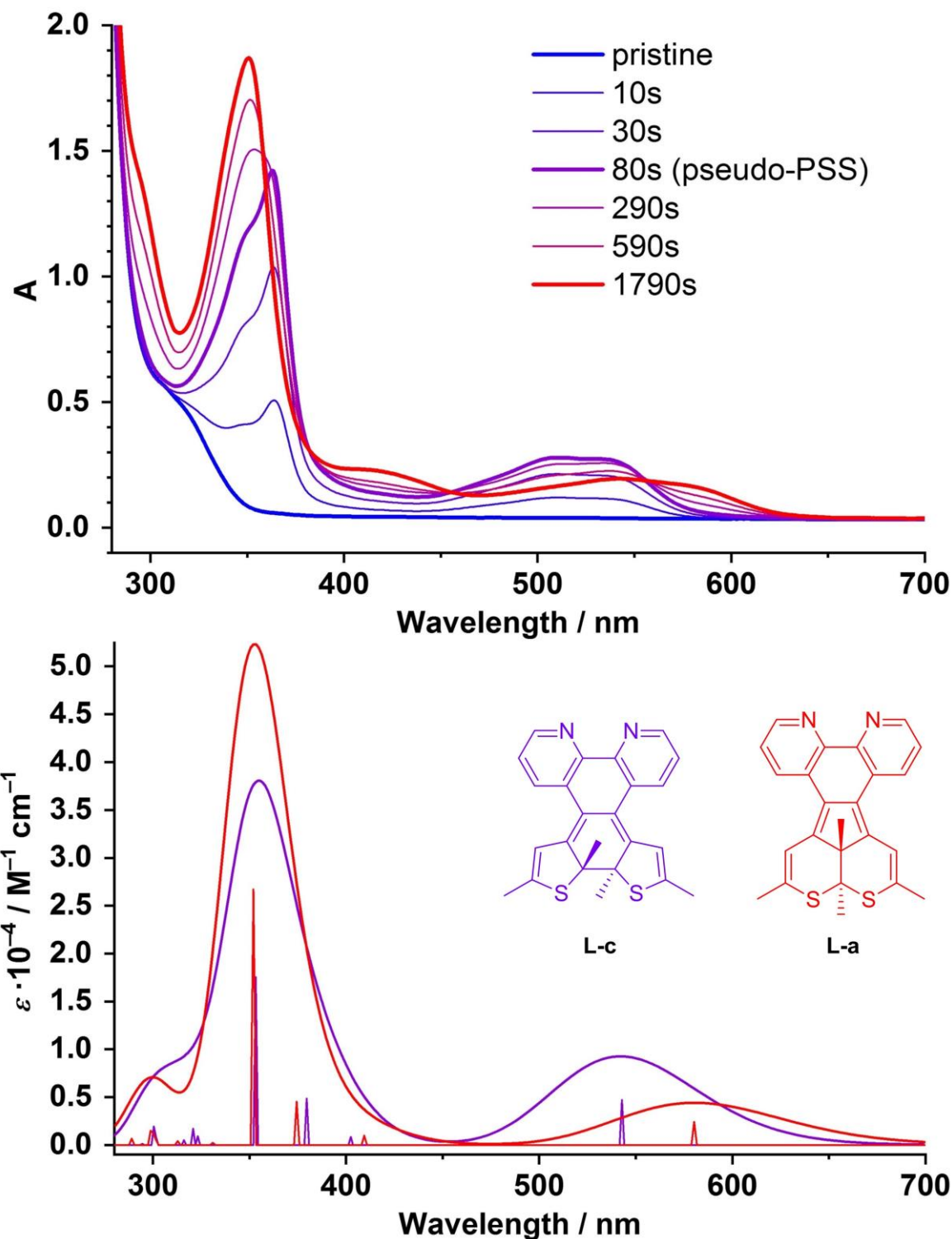


**Figure S27.** (a) Photoresponse of **L-o** to UV irradiation monitored by electronic absorption spectroscopy ( $\lambda = 313$  nm, 15 W, degassed toluene, RT,  $c = 4.5 \times 10^{-5}$  M). (b) Calculated electronic absorption spectra of **L-c** and **L-a** (M05-2x/6-31G(d)/PCM(toluene)//TD-M05/6-31G(d)/PCM(toluene) level of theory).

## IX.2. HOMO and LUMO energies for L-o and L-a

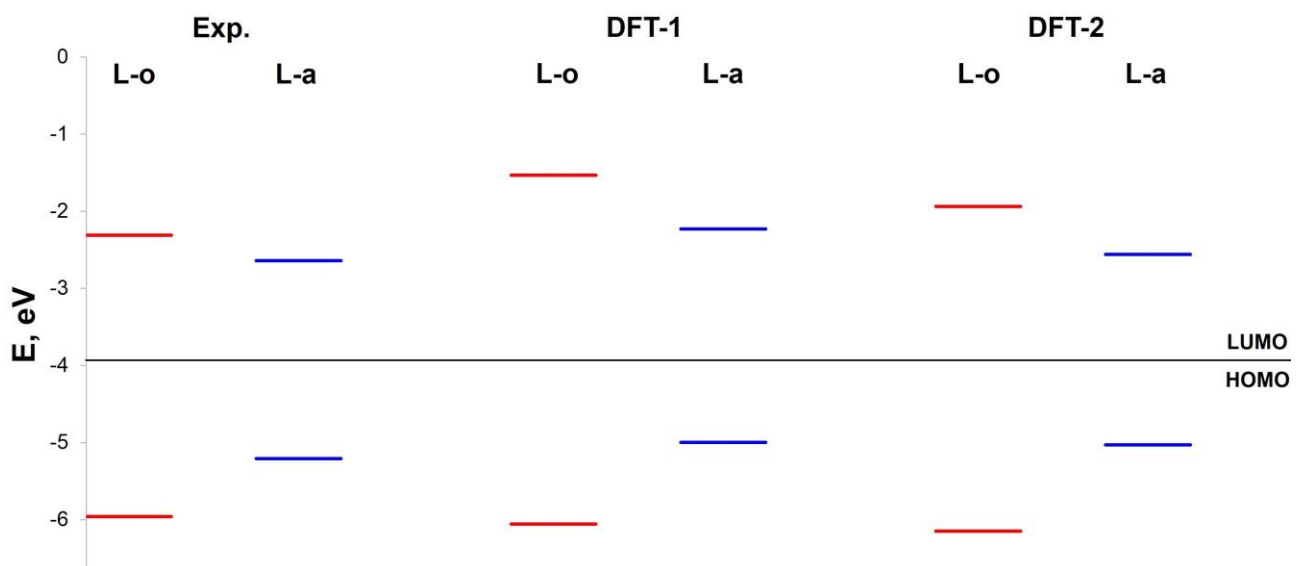
**Table S9.** The energies of frontier molecular orbitals (eV) for **L-o** and **L-a** according to various estimations.

		Experimental values <sup>a</sup>	DFT-1 <sup>b</sup>	DFT-2 <sup>c</sup>
<b>L-o</b>	LUMO	-2.31	-1.53	-1.94
	HOMO	-5.96	-6.06	-6.15
	$\Delta_{\text{LUMO-HOMO}}$	3.65	4.53	4.21
<b>L-a</b>	LUMO	-2.64	-2.23	-2.56
	HOMO	-5.21	-5.00	-5.03
	$\Delta_{\text{LUMO-HOMO}}$	2.57	2.77	2.47

<sup>a</sup> Obtained from cyclic voltammetry, for calculation of these values, see Section V.

<sup>b</sup> PBE0/6-31G(d,p)/PCM(MeCN)

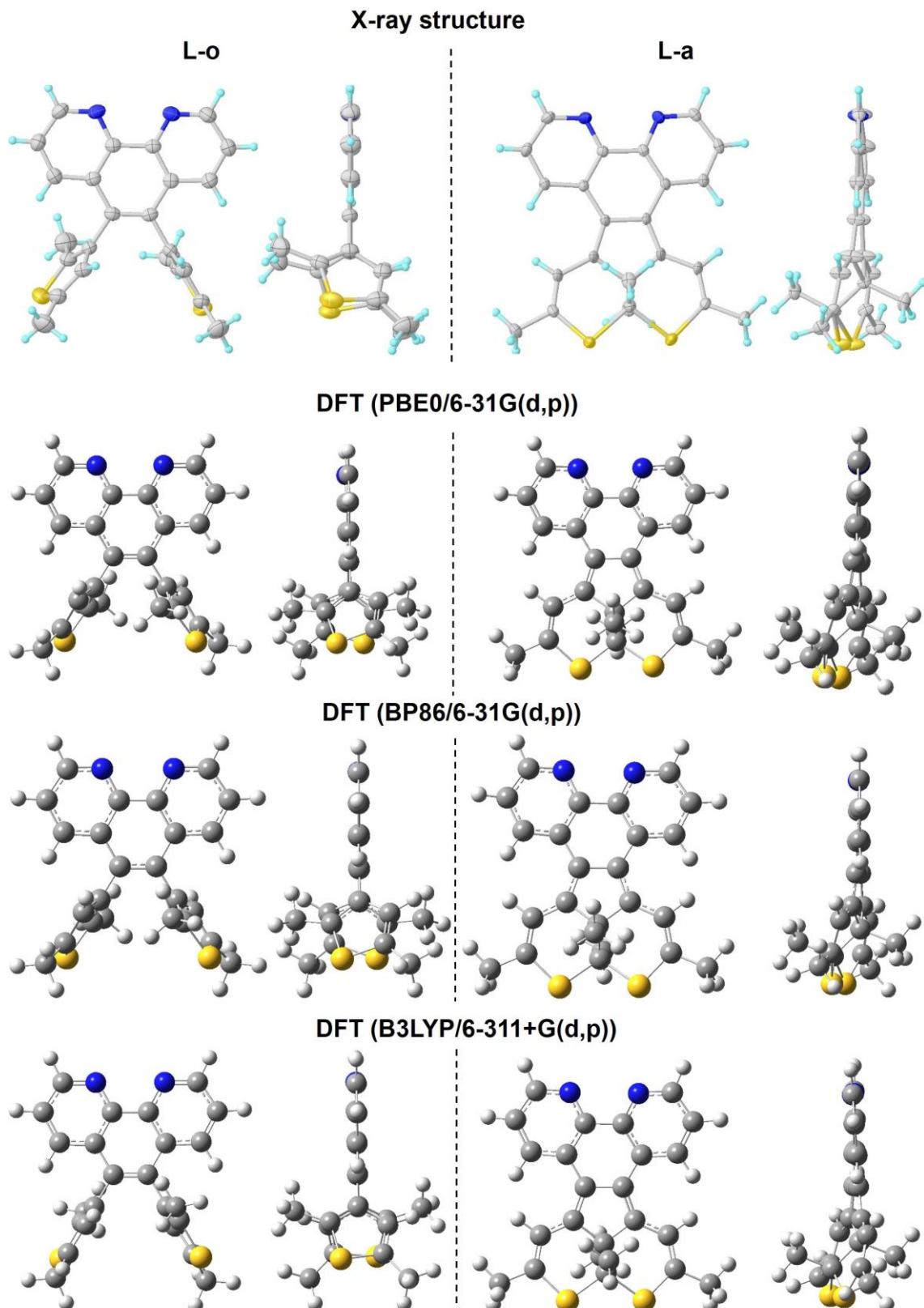
<sup>c</sup> B3LYP/6-311+G(d,p)/PCM(MeCN)



**Figure S28.** The energies of frontier molecular orbitals for **L-o** (red) and **L-a** (blue) according to various estimations (values are given in Table S9).

### IX.3. Comparison of molecular structures of L-o, L-c, and L-a

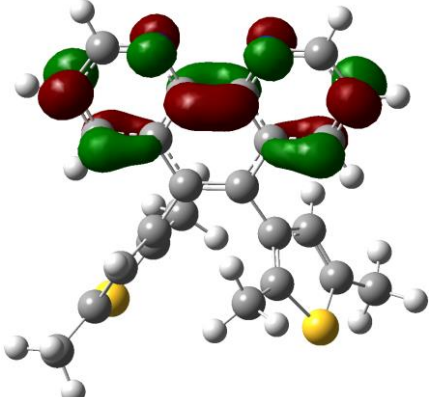
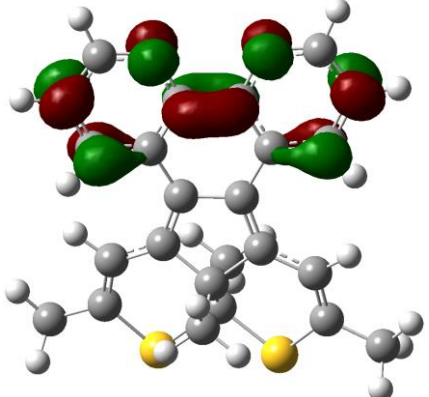
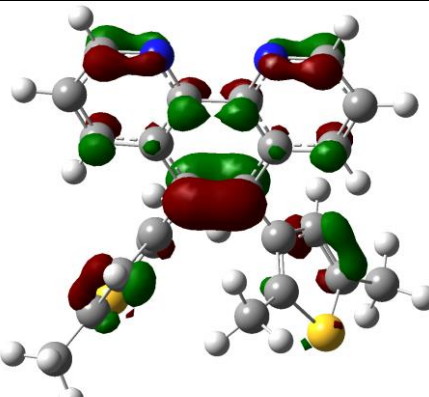
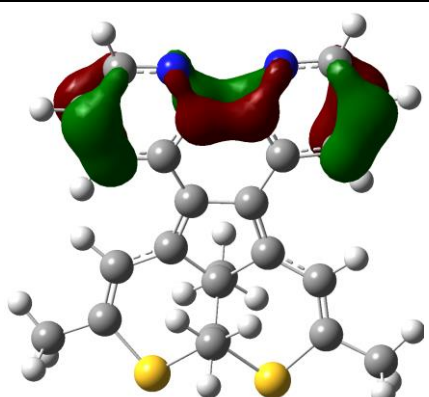
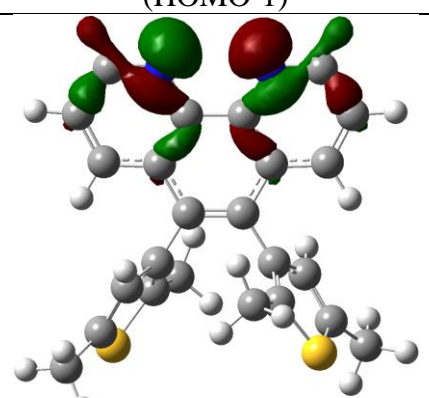
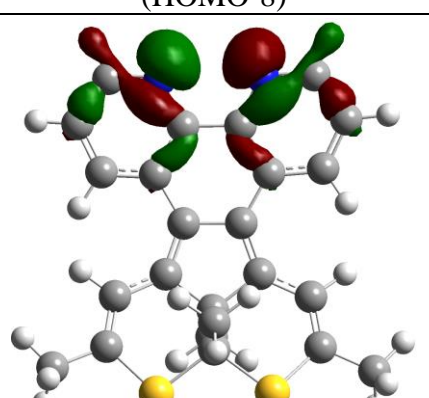
X-ray structure of **L-o** was reported previously.<sup>28</sup>



**Figure S29.** Molecular structures for **L-o** and **L-a** determined experimentally by XRD and by using DFT with different levels of theory.

#### IX.4. Molecular orbitals of L-o and L-a ligands responsible for bonding with an iron(II) ion

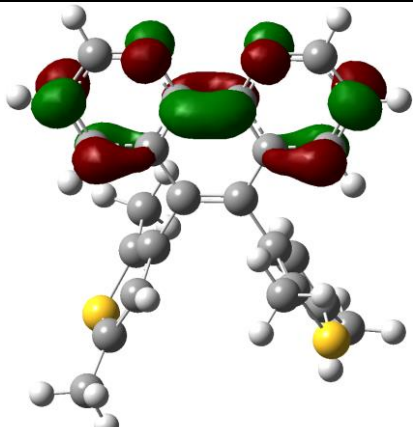
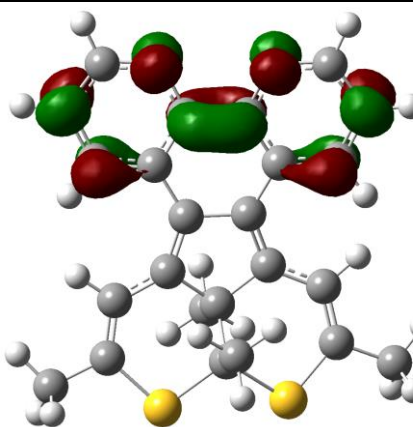
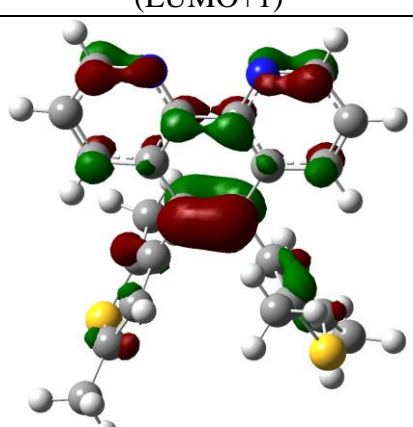
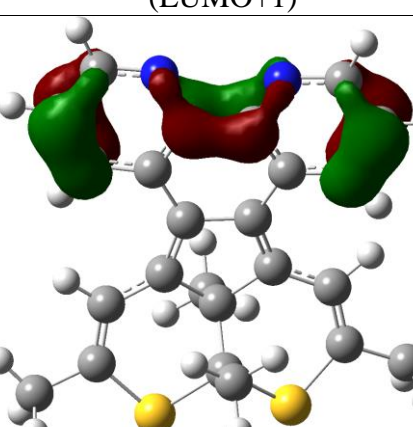
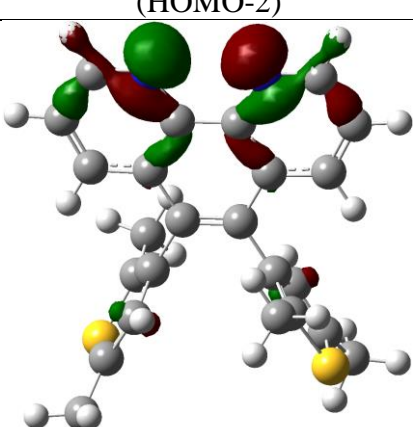
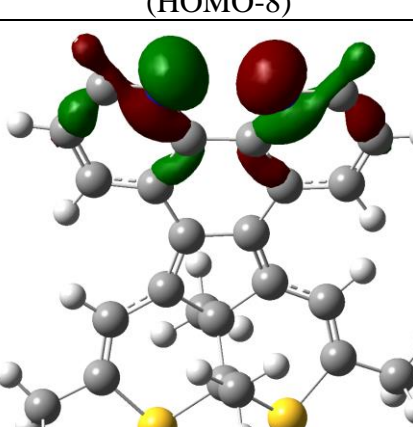
**Table S10.** Molecular orbitals of **L-o** and **L-a** (isovalue: 0.05) according to DFT/PBE0/6-31G(d,p) level of theory.

Type of bonding with a transition metal ion	L-o	L-a
$\pi$ -backbonding		
	-0.04292 E <sub>h</sub> -1.16791 eV (LUMO+1)	-0.04320 E <sub>h</sub> -1.17553 eV (LUMO+1)
$\pi$ -bonding		
	-0.23352 E <sub>h</sub> -6.35441 eV (HOMO-1)	-0.30987 E <sub>h</sub> -8.43200 eV (HOMO-8)
$\sigma$ -bonding		
	-0.24761 E <sub>h</sub> -6.73781 eV (HOMO-3)	-0.24822 E <sub>h</sub> -6.75441 eV (HOMO-2)

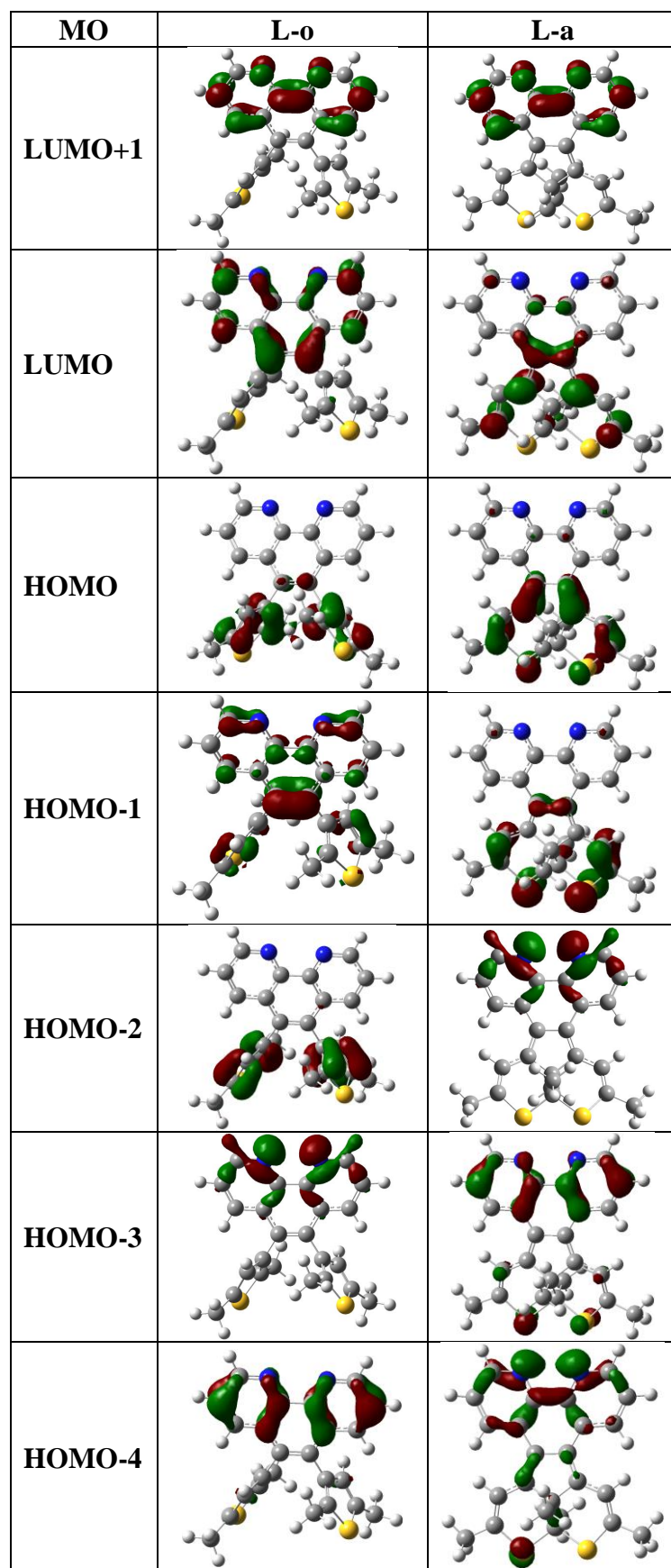
**Table S11.** Molecular orbitals of **L-o** and **L-a** (isovalue: 0.05) according to DFT/BVP86/6-31G(d,p) level of theory.

Type of bonding with a transition metal ion	<b>L-o</b>	<b>L-a</b>
<b><math>\pi</math>-backbonding</b>		
	-0.07739 E <sub>h</sub> -2.10589 eV (LUMO+1)	-0.07756 E <sub>h</sub> -2.11052 eV (LUMO+1)
<b><math>\pi</math>-bonding</b>		
	-0.20166 E <sub>h</sub> -5.48745 eV (HOMO-3)	-0.22836 E <sub>h</sub> -6.21400 eV (HOMO-5)
<b><math>\sigma</math>-bonding</b>		
	-0.19465 E <sub>h</sub> -5.29670 eV (HOMO-1)	-0.19345 E <sub>h</sub> -5.26405 eV (HOMO-1)

**Table S12.** Molecular orbitals of **L-o** and **L-a** (isovalue: 0.05) according to DFT/B3LYP/6-311+G(d,p) level of theory.

Type of bonding with a transition metal ion	L-o	L-a
<b><math>\pi</math>-backbonding</b>		
	-0.06203 E <sub>h</sub> -1.68792 eV (LUMO+1)	-0.06206 E <sub>h</sub> -1.68874 eV (LUMO+1)
<b><math>\pi</math>-bonding</b>		
	-0.23969 E <sub>h</sub> -6.52230 eV (HOMO-2)	-0.30780 E <sub>h</sub> -8.37567 eV (HOMO-8)
<b><math>\sigma</math>-bonding</b>		
	-0.24673 E <sub>h</sub> -6.71387 eV (HOMO-3)	-0.24691 E <sub>h</sub> -6.71877 eV (HOMO-2)

**Table S13.** Symmetry of molecular orbitals of **L-o** and **L-a** (isovalue: 0.05) according to DFT/PBE0/6-31G(d,p) level of theory.



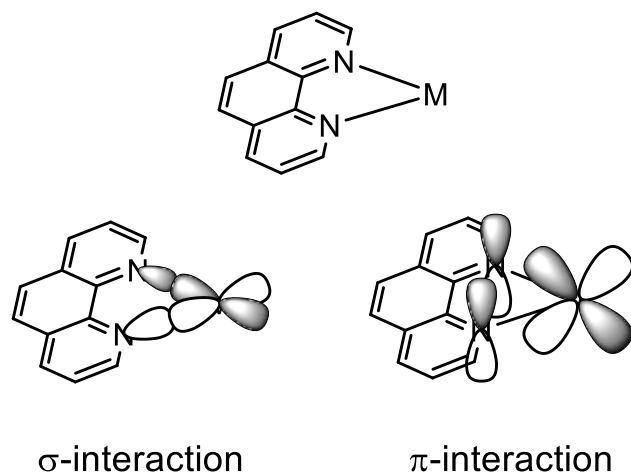
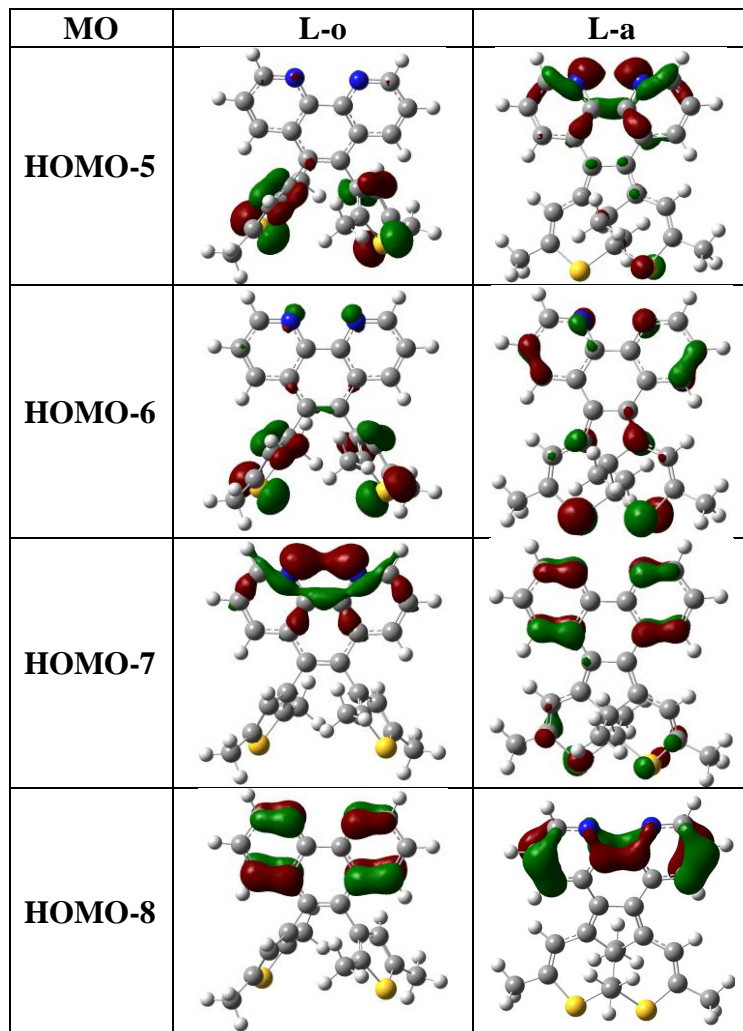


**Figure S30.** Bonding interactions in transition metal complexes with 1,10-phenanthroline ligands.

Note that, LUMO+1, HOMO-1, and HOMO-3 of **L-o** (Figure S29) have a proper symmetry (check Figure S30) to interact with a *d*-metal ion, whereas in case of **L-a**, the proper orbitals are LUMO+1, HOMO-2, and HOMO-8.

## IX.5. Cartesian coordinates of optimized structures

Cartesian coordinate columns of the optimized structure for compound **L-c**  
 (M05-2x/6-31G(d)/PCM(toluene))

1	C	-3.0528430	-0.7027270	-0.2369660
2	C	-3.0528450	0.7027320	0.2369400
3	C	-1.8333470	-1.4027570	-0.3246690
4	C	-0.5689280	-0.7384230	0.0336000
5	C	-1.8333490	1.4027620	0.3246540
6	C	-0.5689270	0.7384270	-0.0336040
7	C	0.5885430	-1.3823760	0.3382910
8	C	1.8521900	-0.5486680	0.5330710
9	C	0.5885480	1.3823770	-0.3382880
10	C	1.8521960	0.5486670	-0.5330560
11	N	-4.2318980	-1.2363880	-0.5686160
12	C	-4.2516520	-2.4824960	-1.0259950
13	C	-1.8823440	-2.6921250	-0.8687780
14	C	-3.1027090	-3.2481360	-1.2126710
15	N	-4.2319020	1.2363910	0.5685830
16	C	-4.2516600	2.4824980	1.0259650
17	C	-1.8823510	2.6921270	0.8687690
18	C	-3.1027180	3.2481360	1.2126550
19	C	0.8564230	-2.7844380	0.5848500
20	C	2.1649960	-3.1080420	0.6236730
21	S	3.2518340	-1.7475010	0.3412600
22	C	0.8564320	2.7844380	-0.5848540
23	C	2.1650060	3.1080390	-0.6236650
24	S	3.2518390	1.7474970	-0.3412320
25	C	2.7525410	-4.4565990	0.8844420
26	C	2.7525570	4.4565960	-0.8844250
27	C	1.8885350	-0.0289100	1.9820730
28	C	1.8885530	0.0289070	-1.9820570
29	H	-5.2268130	-2.8841010	-1.2791210
30	H	-0.9673740	-3.2352490	-1.0570660
31	H	-3.1653670	-4.2409550	-1.6372310
32	H	-5.2268230	2.8841010	1.2790890
33	H	-0.9673820	3.2352490	1.0570700
34	H	-3.1653800	4.2409530	1.6372200
35	H	0.0840030	-3.5175990	0.7692780
36	H	0.0840160	3.5175970	-0.7693000
37	H	3.3799230	-4.7730710	0.0481080
38	H	3.3810720	-4.4352010	1.7773430
39	H	1.9617670	-5.1925140	1.0258590
40	H	3.3811730	4.4351780	-1.7772660
41	H	1.9617850	5.1924950	-1.0259410
42	H	3.3798540	4.7731030	-0.0480410
43	H	2.8180630	0.4995070	2.1859570
44	H	1.0476640	0.6401950	2.1678960
45	H	1.8123940	-0.8846140	2.6537680
46	H	1.8124200	0.8846120	-2.6537530
47	H	2.8180820	-0.4995110	-2.1859320
48	H	1.0476840	-0.6401970	-2.1678880

Cartesian coordinate columns of the optimized structure for compound **L-a**  
(M05-2x/6-31G(d)/PCM(toluene))

1	C	-2.5227330	0.0046710	-0.5011920
2	C	3.2939060	0.6753610	0.0164070
3	C	3.2360350	-0.8028170	-0.1430250
4	C	2.1126190	1.4256410	0.1942730
5	C	0.8226710	0.7410860	0.2089130
6	C	2.0089410	-1.4891460	-0.0258610
7	C	0.7849300	-0.7335260	0.2280760
8	C	-0.4572760	1.2245740	0.2321250
9	C	-1.3843580	0.0692290	0.5182710
10	C	-0.5042570	-1.1491450	0.3998040
11	N	4.5106690	1.2298310	-0.0020020
12	C	4.6136950	2.5398700	0.1731730
13	C	2.2609400	2.7986770	0.4292000
14	C	3.5193430	3.3705360	0.4095290
15	N	4.3936820	-1.4215970	-0.3998050
16	C	4.3858360	-2.7375920	-0.5633770
17	C	2.0296640	-2.8731120	-0.2437480
18	C	3.2277230	-3.5112800	-0.5060600
19	C	-1.0253080	2.5312760	0.0023340
20	C	-2.3375980	2.7520120	-0.2383340
21	S	-3.5841480	1.5023480	-0.3179360
22	S	-3.6209740	-1.4315320	-0.1434970
23	C	-1.1261050	-2.4464440	0.5269160
24	C	-2.4482230	-2.6561150	0.3488670
25	C	-2.8890990	4.1262080	-0.4968570
26	C	-3.0927090	-3.9983950	0.5565220
27	C	-1.8414950	0.1981250	1.9903660
28	C	-2.0221370	-0.0922010	-1.9444920
29	H	5.6176660	2.9492390	0.1433570
30	H	1.4018510	3.4084970	0.6613530
31	H	3.6571770	4.4282230	0.5879890
32	H	5.3456550	-3.2003760	-0.7657830
33	H	1.1118980	-3.4396890	-0.2410160
34	H	3.2676270	-4.5781700	-0.6786880
35	H	-0.3831520	3.3974520	-0.0712990
36	H	-0.5378180	-3.3031850	0.8297440
37	H	-3.3007360	4.1927690	-1.5062810
38	H	-3.6950820	4.3605020	0.2031060
39	H	-2.1057750	4.8750480	-0.3820180
40	H	-3.5610530	-4.3505540	-0.3652430
41	H	-2.3473120	-4.7270390	0.8741200
42	H	-3.8707710	-3.9413150	1.3215410
43	H	-2.4013190	1.1194160	2.1447270
44	H	-2.4604960	-0.6513750	2.2778590
45	H	-0.9512920	0.2151600	2.6202260
46	H	-2.8713980	-0.1383180	-2.6243520
47	H	-1.4157780	0.7799770	-2.1926510
48	H	-1.4184320	-0.9919080	-2.0720930

Cartesian coordinate columns of the optimized structure for compound **L-o**  
(PBE0/6-31G(d,p)/PCM(MeCN))

1	N	4.1998920	-1.3628620	0.1081910
2	C	3.0124430	-0.7239560	0.0542100
3	C	4.1967480	-2.6786800	0.2171060
4	C	1.7711500	-1.4069360	0.1037430
5	C	3.0289050	-3.4546580	0.2876950
6	C	1.8137880	-2.8114920	0.2334860
7	C	3.0124400	0.7239410	-0.0542330
8	C	1.7711430	1.4069170	-0.1037500
9	C	0.5196250	-0.6849290	0.0504560
10	C	0.5196230	0.6849070	-0.0504450
11	N	4.1998850	1.3628530	-0.1082270
12	C	4.1967330	2.6786710	-0.2171410
13	C	1.8137730	2.8114730	-0.2334910
14	C	3.0288870	3.4546450	-0.2877140
15	C	-0.7455880	-1.4609160	0.1098890
16	C	-1.5490440	-1.5379680	1.2197270
17	C	-1.2354270	-2.2504300	-0.9834390
18	S	-2.9166030	-2.5611730	0.9046100
19	C	-2.4039750	-2.9030390	-0.7197780
20	C	-0.7455900	1.4608950	-0.1098710
21	C	-1.2353860	2.2504620	0.9834380
22	C	-1.5490460	1.5379580	-1.2197080
23	C	-2.4038980	2.9031300	0.7197590
24	S	-2.9166860	2.5610350	-0.9045290
25	C	-3.1963090	-3.7938780	-1.6176000
26	C	-1.3758650	-0.8902520	2.5529300
27	C	-1.3758650	0.8902600	-2.5529190
28	C	-3.1961360	3.7941060	1.6175290
29	H	5.1716940	-3.1627370	0.2561370
30	H	3.0928460	-4.5332140	0.3859870
31	H	0.8851230	-3.3700780	0.2887080
32	H	5.1716770	3.1627330	-0.2561840
33	H	0.8851050	3.3700550	-0.2886990
34	H	3.0928220	4.5332010	-0.3860040
35	H	-0.7278090	-2.3203190	-1.9401760
36	H	-0.7277290	2.3204030	1.9401500
37	H	-3.3077420	-4.7997820	-1.1992760
38	H	-4.2024520	-3.4008580	-1.7978670
39	H	-2.6916340	-3.8838540	-2.5827160
40	H	-1.5036820	-1.6068970	3.3701570
41	H	-0.3732360	-0.4624360	2.6291310
42	H	-2.0957040	-0.0787210	2.7044210
43	H	-0.3732180	0.4624920	-2.6291480
44	H	-2.0956700	0.0786960	-2.7043930
45	H	-1.5037380	1.6069010	-3.3701420
46	H	-2.6913920	3.8841780	2.5826010
47	H	-3.3075640	4.7999660	1.1990970
48	H	-4.2022790	3.4011420	1.7979110

Cartesian coordinate columns of the optimized structure for compound **L-o**

(B3LYP/6-311+G(d,p)/PCM(MeCN))

1	N	4.2026640	-1.3784630	-0.0505070
2	C	3.0166160	-0.7274270	-0.0188140
3	C	4.1996430	-2.7004870	-0.0881290
4	C	1.7717130	-1.4135370	-0.0227470
5	C	3.0272060	-3.4748970	-0.0992590
6	C	1.8134730	-2.8257060	-0.0663510
7	C	3.0166260	0.7274170	0.0188400
8	C	1.7717320	1.4135430	0.0227890
9	C	0.5191510	-0.6862810	-0.0002720
10	C	0.5191590	0.6863020	0.0003450
11	N	4.2026840	1.3784350	0.0504990
12	C	4.1996830	2.7004600	0.0881110
13	C	1.8135140	2.8257120	0.0663760
14	C	3.0272570	3.4748870	0.0992580
15	C	-0.7608280	-1.4551250	-0.0104040
16	C	-1.3241520	-2.0232100	1.1022900
17	C	-1.5195680	-1.6973640	-1.2083360
18	S	-2.8057360	-2.8556960	0.6759180
19	C	-2.6497550	-2.4354610	-1.0176450
20	C	-0.7608140	1.4551580	0.0104400
21	C	-1.5195750	1.6974260	1.2083530
22	C	-1.3241410	2.0231800	-1.1022840
23	C	-2.6498060	2.4354410	1.0176090
24	S	-2.8056330	2.8558400	-0.6759290
25	C	-3.6664620	-2.8738980	-2.0272070
26	C	-0.8457030	-2.0050770	2.5225040
27	C	-0.8457080	2.0049480	-2.5225020
28	C	-3.6666040	2.8737840	2.0271200
29	H	5.1715910	-3.1863080	-0.1129520
30	H	3.0876340	-4.5557500	-0.1344820
31	H	0.8873710	-3.3860170	-0.0754390
32	H	5.1716380	3.1862670	0.1129050
33	H	0.8874210	3.3860370	0.0754800
34	H	3.0877010	4.5557390	0.1344700
35	H	-1.2220700	-1.3251470	-2.1810270
36	H	-1.2221070	1.3252130	2.1810550
37	H	-3.7455580	-3.9639430	-2.0773710
38	H	-4.6622700	-2.4832180	-1.7975300
39	H	-3.3816180	-2.5107060	-3.0166710
40	H	-0.6201240	-3.0122330	2.8862630
41	H	0.0631930	-1.4068820	2.6053510
42	H	-1.5936800	-1.5739210	3.1943710
43	H	0.0630970	1.4066140	-2.6053460
44	H	-1.5937540	1.5738910	-3.1943560
45	H	-0.6199830	3.0120650	-2.8862800
46	H	-3.3818210	2.5105440	3.0165840
47	H	-3.7457320	3.9638240	2.0773390
48	H	-4.6623850	2.4830910	1.7973490

Cartesian coordinate columns of the optimized structure for compound **L-a**  
(PBE0/6-31G(d,p)/PCM(MeCN))

1	C	-2.5423100	0.0021530	-0.4963610
2	C	3.2969000	0.6830570	0.0104320
3	C	3.2485950	-0.7900000	-0.1351060
4	C	2.1050810	1.4281130	0.1791110
5	C	0.8254350	0.7360460	0.1926660
6	C	2.0188010	-1.4837220	-0.0292660
7	C	0.7930800	-0.7341690	0.2034530
8	C	-0.4633750	1.2188860	0.2165030
9	C	-1.3823100	0.0577900	0.5013600
10	C	-0.5034300	-1.1593240	0.3633250
11	N	4.5107910	1.2510470	-0.0112480
12	C	4.6038870	2.5650660	0.1506670
13	C	2.2470020	2.8074460	0.3971090
14	C	3.5013800	3.3884670	0.3755200
15	N	4.4138640	-1.4099320	-0.3664050
16	C	4.4177700	-2.7289690	-0.5134240
17	C	2.0571790	-2.8732830	-0.2263250
18	C	3.2628180	-3.5078500	-0.4624490
19	C	-1.0281870	2.5176930	-0.0025650
20	C	-2.3490880	2.7551870	-0.2156820
21	S	-3.5947040	1.5072430	-0.2750500
22	S	-3.6310280	-1.4399620	-0.1163590
23	C	-1.1172290	-2.4513720	0.4691590
24	C	-2.4480150	-2.6720190	0.3213800
25	C	-2.8941620	4.1296350	-0.4519590
26	C	-3.0731290	-4.0202150	0.5073230
27	C	-1.8140840	0.1706570	1.9819280
28	C	-2.0863110	-0.0855370	-1.9526890
29	H	5.6074510	2.9859770	0.1182400
30	H	1.3821630	3.4200660	0.6155300
31	H	3.6290140	4.4528120	0.5421470
32	H	5.3862110	-3.1920290	-0.6954350
33	H	1.1437260	-3.4527110	-0.2240610
34	H	3.3102130	-4.5804680	-0.6178980
35	H	-0.3818360	3.3841680	-0.0891240
36	H	-0.5185290	-3.3214190	0.7205080
37	H	-3.3378690	4.2123790	-1.4503240
38	H	-3.6805810	4.3752270	0.2711020
39	H	-2.1011930	4.8750520	-0.3563790
40	H	-3.5643270	-4.3595440	-0.4113450
41	H	-2.3137980	-4.7536590	0.7879290
42	H	-3.8364740	-3.9993250	1.2933830
43	H	-2.3905900	1.0818690	2.1547270
44	H	-2.4131100	-0.6931340	2.2798070
45	H	-0.9162020	0.2021670	2.6042450
46	H	-2.9531450	-0.1330860	-2.6143180
47	H	-1.4898270	0.7911140	-2.2197650
48	H	-1.4799520	-0.9821710	-2.1075140

Cartesian coordinate columns of the optimized structure for compound **L-a**

(B3LYP/6-311+G(d,p)/PCM(MeCN))

1	C	2.5462010	0.0015150	-0.5039170
2	C	-3.2537080	-0.7952390	-0.1417480
3	C	-3.3054040	0.6823590	0.0078890
4	C	-2.0212510	-1.4892570	-0.0198380
5	C	-0.7931310	-0.7372190	0.2180460
6	C	-2.1118350	1.4302960	0.1800910
7	C	-0.8272100	0.7393500	0.1990050
8	C	0.5049170	-1.1619120	0.3806630
9	C	1.3894470	0.0618200	0.5093330
10	C	0.4614890	1.2260470	0.2249830
11	N	-4.4143430	-1.4242790	-0.3901300
12	C	-4.4182550	-2.7462870	-0.5339150
13	C	-2.0600800	-2.8832970	-0.2034500
14	C	-3.2617430	-3.5218860	-0.4550340
15	N	-4.5199880	1.2566280	-0.0113370
16	C	-4.6177010	2.5725350	0.1529450
17	C	-2.2570780	2.8127310	0.3931610
18	C	-3.5122830	3.3946110	0.3738380
19	C	1.1204920	-2.4571100	0.4784750
20	C	2.4491060	-2.6898910	0.3252450
21	S	3.6485850	-1.4543320	-0.1147250
22	S	3.6041740	1.5307060	-0.3044140
23	C	1.0241650	2.5295700	0.0090480
24	C	2.3413560	2.7793490	-0.2148460
25	C	3.0666250	-4.0494110	0.5033010
26	C	2.8792530	4.1652520	-0.4403490
27	C	1.8358140	0.1819410	1.9972970
28	C	2.0899310	-0.1024330	-1.9672900
29	H	-5.3811380	-3.2088250	-0.7319260
30	H	-1.1528160	-3.4658560	-0.1741790
31	H	-3.3052020	-4.5943110	-0.6002450
32	H	-5.6199330	2.9907880	0.1238740
33	H	-1.3961510	3.4289320	0.6017950
34	H	-3.6388110	4.4576740	0.5379290
35	H	0.5181360	-3.3238210	0.7206510
36	H	0.3756040	3.3932840	-0.0525250
37	H	3.5469580	-4.3901620	-0.4192390
38	H	3.8347950	-4.0372060	1.2832730
39	H	2.3035020	-4.7757870	0.7872770
40	H	3.3106280	4.2633630	-1.4415370
41	H	2.0834970	4.9034580	-0.3276710
42	H	3.6706170	4.4057740	0.2771860
43	H	2.4378980	-0.6759410	2.2970180
44	H	2.4115800	1.0918950	2.1643940
45	H	0.9441780	0.2147620	2.6258030
46	H	2.9575330	-0.1448570	-2.6256460
47	H	1.4952890	-1.0048820	-2.1213340
48	H	1.4852950	0.7626820	-2.2460000

Cartesian coordinate columns of the optimized structure for compound **L-o**  
(PBE0/6-31G(d,p))

1	N	-4.1986390	1.3548740	0.1305050
2	C	-3.0111260	0.7229130	0.0652040
3	C	-4.1985640	2.6659210	0.2620790
4	C	-1.7699790	1.4060440	0.1233320
5	C	-3.0327870	3.4444640	0.3479790
6	C	-1.8152720	2.8074130	0.2810380
7	C	-3.0111350	-0.7229090	-0.0651940
8	C	-1.7699970	-1.4060560	-0.1233190
9	C	-0.5178970	0.6849080	0.0567820
10	C	-0.5179040	-0.6849340	-0.0567560
11	N	-4.1986570	-1.3548520	-0.1305110
12	C	-4.1986000	-2.6658970	-0.2620980
13	C	-1.8153090	-2.8074230	-0.2810440
14	C	-3.0328330	-3.4444560	-0.3479990
15	C	0.7447200	1.4648540	0.1149000
16	C	1.5837950	1.5041530	1.2000280
17	C	1.1960590	2.3050640	-0.9561390
18	S	2.9330030	2.5489990	0.8889090
19	C	2.3675920	2.9552030	-0.6999610
20	C	0.7447090	-1.4648840	-0.1148890
21	C	1.1960620	-2.3051010	0.9561390
22	C	1.5838110	-1.5041160	-1.1999980
23	C	2.3676020	-2.9552240	0.6999500
24	S	2.9329590	-2.5490610	-0.8889500
25	C	3.1247820	3.8900310	-1.5833950
26	C	1.4561410	0.7994970	2.5087510
27	C	1.4561910	-0.7993670	-2.5086750
28	C	3.1248170	-3.8900350	1.5833790
29	H	-5.1767460	3.1436860	0.3091670
30	H	-3.0992130	4.5211440	0.4690850
31	H	-0.8870590	3.3656220	0.3500520
32	H	-5.1767890	-3.1436470	-0.3092000
33	H	-0.8871060	-3.3656450	-0.3500610
34	H	-3.0992740	-4.5211330	-0.4691180
35	H	0.6562380	2.4124280	-1.8917170
36	H	0.6562520	-2.4124700	1.8917230
37	H	3.2403770	4.8798400	-1.1286070
38	H	4.1281940	3.5145120	-1.8115550
39	H	2.5911590	4.0162780	-2.5290130
40	H	1.6400860	1.4744050	3.3506340
41	H	0.4459960	0.3952630	2.6116390
42	H	2.1590950	-0.0371460	2.5857840
43	H	0.4460560	-0.3951050	-2.6115480
44	H	2.1591640	0.0372670	-2.5856480
45	H	1.6401330	-1.4742240	-3.3505980
46	H	2.5912190	-4.0162680	2.5290140
47	H	3.2404010	-4.8798510	1.1286030
48	H	4.1282350	-3.5145120	1.8115080

Cartesian coordinate columns of the optimized structure for compound **L-o**  
(BVP86/6-31G(d,p))

1	N	4.2338780	-1.3649840	0.1198490
2	C	3.0333570	-0.7273160	0.0600370
3	C	4.2281080	-2.6917960	0.2438300
4	C	1.7782320	-1.4179840	0.1150120
5	C	3.0530050	-3.4741940	0.3271180
6	C	1.8255790	-2.8304490	0.2651390
7	C	3.0333490	0.7273460	-0.0600140
8	C	1.7782150	1.4179970	-0.1150180
9	C	0.5186500	-0.6932500	0.0538770
10	C	0.5186420	0.6932450	-0.0539210
11	N	4.2338620	1.3650310	-0.1197900
12	C	4.2280770	2.6918430	-0.2437660
13	C	1.8255470	2.8304640	-0.2651370
14	C	3.0529660	3.4742250	-0.3270810
15	C	-0.7517900	-1.4773920	0.1131210
16	C	-1.5881370	-1.5265880	1.2180620
17	C	-1.2118490	-2.3176480	-0.9646870
18	S	-2.9526450	-2.5869830	0.9089110
19	C	-2.3896990	-2.9824650	-0.7064280
20	C	-0.7518080	1.4773710	-0.1131540
21	C	-1.2119250	2.3175270	0.9647080
22	C	-1.5881100	1.5266530	-1.2181270
23	C	-2.3897750	2.9823460	0.7064610
24	S	-2.9526510	2.5869950	-0.9089340
25	C	-3.1540030	-3.9199490	-1.5953250
26	C	-1.4517070	-0.8310560	2.5404300
27	C	-1.4516080	0.8312590	-2.5405590
28	C	-3.1541320	3.9197380	1.5954100
29	H	5.2132770	-3.1748610	0.2860970
30	H	3.1173090	-4.5600320	0.4423120
31	H	0.8902730	-3.3920150	0.3314280
32	H	5.2132410	3.1749220	-0.2860040
33	H	0.8902360	3.3920180	-0.3314490
34	H	3.1172580	4.5600650	-0.4422690
35	H	-0.6746780	-2.4174970	-1.9113450
36	H	-0.6747950	2.4172990	1.9113970
37	H	-3.2629960	-4.9224800	-1.1464870
38	H	-4.1694990	-3.5481970	-1.8165180
39	H	-2.6236750	-4.0374680	-2.5532710
40	H	-1.6416180	-1.5144970	3.3847430
41	H	-0.4304010	-0.4342230	2.6462710
42	H	-2.1501160	0.0189340	2.6301950
43	H	-0.4302880	0.4344610	-2.6463960
44	H	-2.1499930	-0.0187380	-2.6304410
45	H	-1.6414980	1.5147830	-3.3848100
46	H	-2.6238440	4.0371810	2.5533880
47	H	-3.2631230	4.9223070	1.1466580
48	H	-4.1696290	3.5479480	1.8165290

Cartesian coordinate columns of the optimized structure for compound **L-o**  
(B3LYP/6-311+G(d,p))

1	N	-4.2050260	-1.3721890	0.0289140
2	C	-3.0187980	-0.7276210	0.0117610
3	C	-4.2048380	-2.6913300	0.0575490
4	C	-1.7738040	-1.4146600	0.0168180
5	C	-3.0344040	-3.4707310	0.0744310
6	C	-1.8177000	-2.8266220	0.0533720
7	C	-3.0187970	0.7276280	-0.0117570
8	C	-1.7738010	1.4146650	-0.0168170
9	C	-0.5216340	-0.6864110	-0.0002730
10	C	-0.5216330	0.6864130	0.0002710
11	N	-4.2050230	1.3721990	-0.0289090
12	C	-4.2048330	2.6913400	-0.0575440
13	C	-1.8176940	2.8266280	-0.0533710
14	C	-3.0343970	3.4707390	-0.0744280
15	C	0.7593940	-1.4538180	0.0101890
16	C	1.3364930	-2.0040800	-1.1044290
17	C	1.5076900	-1.7147030	1.2089890
18	S	2.8147300	-2.8396760	-0.6796480
19	C	2.6410650	-2.4464840	1.0159970
20	C	0.7593980	1.4538170	-0.0101910
21	C	1.5076910	1.7147050	-1.2089920
22	C	1.3365040	2.0040670	1.1044290
23	C	2.6410650	2.4464880	-1.0160010
24	S	2.8147400	2.8396640	0.6796470
25	C	3.6510720	-2.8946710	2.0277720
26	C	0.8733810	-1.9580160	-2.5290970
27	C	0.8734000	1.9579910	2.5290990
28	C	3.6510660	2.8946850	-2.0277780
29	H	-5.1803120	-3.1720800	0.0702940
30	H	-3.0980240	-4.5522280	0.1046330
31	H	-0.8915850	-3.3874600	0.0676510
32	H	-5.1803060	3.1720920	-0.0702870
33	H	-0.8915780	3.3874630	-0.0676530
34	H	-3.0980150	4.5522360	-0.1046300
35	H	1.1990450	-1.3591020	2.1843460
36	H	1.1990430	1.3591100	-2.1843500
37	H	3.7457690	-3.9845260	2.0548540
38	H	4.6438020	-2.4826440	1.8218840
39	H	3.3494050	-2.5601070	3.0226220
40	H	0.6985790	-2.9601980	-2.9327420
41	H	-0.0625590	-1.4014170	-2.6010270
42	H	1.6076110	-1.4679250	-3.1763650
43	H	-0.0625440	1.4013990	2.6010280
44	H	1.6076300	1.4678870	3.1763570
45	H	0.6986090	2.9601700	2.9327560
46	H	3.3493940	2.5601290	-3.0226280
47	H	3.7457620	3.9845410	-2.0548510
48	H	4.6437980	2.4826570	-1.8218980

Cartesian coordinate columns of the optimized structure for compound **L-a**  
(PBE0/6-31G(d,p))

1	C	-2.5444640	0.0040290	-0.4891920
2	C	3.2975970	0.6798350	0.0129450
3	C	3.2477140	-0.7919960	-0.1392620
4	C	2.1066450	1.4249030	0.1864720
5	C	0.8266660	0.7344140	0.1949310
6	C	2.0171350	-1.4848570	-0.0355130
7	C	0.7926520	-0.7353980	0.2035180
8	C	-0.4615080	1.2176910	0.2164360
9	C	-1.3824770	0.0597260	0.5057650
10	C	-0.5039190	-1.1574440	0.3670430
11	N	4.5109350	1.2427510	-0.0063800
12	C	4.6063600	2.5526490	0.1649080
13	C	2.2507430	2.8009270	0.4180680
14	C	3.5067000	3.3781520	0.4002690
15	N	4.4116490	-1.4074980	-0.3742390
16	C	4.4150770	-2.7229180	-0.5289650
17	C	2.0543470	-2.8720240	-0.2435700
18	C	3.2603120	-3.5036930	-0.4847900
19	C	-1.0232900	2.5144300	-0.0184560
20	C	-2.3438230	2.7519970	-0.2337710
21	S	-3.5948280	1.5113640	-0.2685530
22	S	-3.6350400	-1.4361090	-0.1078860
23	C	-1.1198990	-2.4479030	0.4744800
24	C	-2.4513970	-2.6648280	0.3281330
25	C	-2.8822110	4.1253490	-0.4940250
26	C	-3.0774900	-4.0126930	0.5185470
27	C	-1.8139480	0.1757110	1.9860580
28	C	-2.0916880	-0.0861890	-1.9464320
29	H	5.6123170	2.9687570	0.1327470
30	H	1.3844580	3.4084860	0.6477790
31	H	3.6385770	4.4405820	0.5790750
32	H	5.3854220	-3.1818550	-0.7133250
33	H	1.1374900	-3.4470430	-0.2495400
34	H	3.3084240	-4.5752820	-0.6507550
35	H	-0.3694070	3.3735560	-0.1254320
36	H	-0.5194990	-3.3163380	0.7292740
37	H	-3.3314500	4.1912690	-1.4912710
38	H	-3.6631230	4.3904680	0.2284980
39	H	-2.0854110	4.8694780	-0.4170530
40	H	-3.5714750	-4.3535410	-0.3982740
41	H	-2.3192200	-4.7476230	0.7996360
42	H	-3.8389480	-3.9900760	1.3066550
43	H	-2.3922050	1.0861120	2.1563360
44	H	-2.4143350	-0.6867800	2.2845940
45	H	-0.9151090	0.2080750	2.6068370
46	H	-2.9611540	-0.1339930	-2.6044580
47	H	-1.4942950	0.7892290	-2.2153670
48	H	-1.4862540	-0.9835640	-2.1001810

Cartesian coordinate columns of the optimized structure for compound **L-a**  
 (BPV86/6-31G(d,p))

1	C	-2.5745750	0.0033000	-0.4882180
2	C	3.3280360	0.6856210	0.0135320
3	C	3.2822510	-0.7916880	-0.1404290
4	C	2.1198200	1.4322590	0.1878020
5	C	0.8389970	0.7351280	0.1857610
6	C	2.0366940	-1.4918790	-0.0489640
7	C	0.8064400	-0.7415600	0.1844540
8	C	-0.4669800	1.2255900	0.2030500
9	C	-1.3927610	0.0549670	0.4972240
10	C	-0.5076210	-1.1733540	0.3446370
11	N	4.5527540	1.2601050	-0.0041510
12	C	4.6356000	2.5843170	0.1726360
13	C	2.2588500	2.8197530	0.4280750
14	C	3.5215220	3.4077500	0.4146260
15	N	4.4626200	-1.4130510	-0.3647080
16	C	4.4614400	-2.7424480	-0.5205130
17	C	2.0778350	-2.8905950	-0.2612330
18	C	3.2953610	-3.5271330	-0.4919310
19	C	-1.0242140	2.5231250	-0.0386090
20	C	-2.3613300	2.7813770	-0.2363110
21	S	-3.6346940	1.5401590	-0.2412300
22	S	-3.6763070	-1.4613060	-0.0882990
23	C	-1.1196620	-2.4661100	0.4503360
24	C	-2.4690370	-2.6960800	0.3318890
25	C	-2.8889970	4.1670360	-0.5057330
26	C	-3.0856260	-4.0574270	0.5299070
27	C	-1.8088050	0.1639960	1.9980820
28	C	-2.1594240	-0.0826690	-1.9669430
29	H	5.6460360	3.0115560	0.1396740
30	H	1.3815600	3.4240970	0.6636280
31	H	3.6471560	4.4779820	0.6020370
32	H	5.4405640	-3.2072150	-0.6936210
33	H	1.1532050	-3.4682040	-0.2807580
34	H	3.3431200	-4.6065800	-0.6618270
35	H	-0.3563920	3.3784760	-0.1747760
36	H	-0.5056230	-3.3430290	0.6783060
37	H	-3.3603930	4.2317840	-1.5020990
38	H	-3.6577630	4.4588800	0.2320800
39	H	-2.0740030	4.9056060	-0.4524910
40	H	-3.6036810	-4.4028420	-0.3819970
41	H	-2.3094930	-4.7934710	0.7903730
42	H	-3.8338280	-4.0495070	1.3422260
43	H	-2.3968210	1.0751120	2.1791430
44	H	-2.4009680	-0.7113190	2.3036810
45	H	-0.8962240	0.2029890	2.6116670
46	H	-3.0516410	-0.1323590	-2.6069700
47	H	-1.5681070	0.8014040	-2.2522580
48	H	-1.5511910	-0.9840310	-2.1402810

Cartesian coordinate columns of the optimized structure for compound **L-a**

(B3LYP/6-311+G(d,p))

1	C	2.5485180	0.0030820	-0.4973500
2	C	-3.2530890	-0.7961510	-0.1441220
3	C	-3.3054920	0.6804730	0.0089830
4	C	-2.0202360	-1.4901760	-0.0254880
5	C	-0.7925890	-0.7382700	0.2167480
6	C	-2.1128310	1.4285590	0.1857900
7	C	-0.8277840	0.7384300	0.2010130
8	C	0.5053800	-1.1604300	0.3827300
9	C	1.3900180	0.0628110	0.5134800
10	C	0.4606490	1.2247270	0.2259710
11	N	-4.4139290	-1.4185040	-0.3919600
12	C	-4.4194940	-2.7365360	-0.5412320
13	C	-2.0600280	-2.8821990	-0.2185290
14	C	-3.2638580	-3.5162070	-0.4713980
15	N	-4.5198340	1.2479370	-0.0109710
16	C	-4.6206640	2.5593340	0.1602370
17	C	-2.2613060	2.8080920	0.4101070
18	C	-3.5187750	3.3850040	0.3921160
19	C	1.1227650	-2.4545990	0.4810090
20	C	2.4518370	-2.6844610	0.3279530
21	S	3.6521000	-1.4517910	-0.1095550
22	S	3.6061600	1.5327630	-0.2961980
23	C	1.0218250	2.5264210	-0.0025680
24	C	2.3388830	2.7757190	-0.2278120
25	C	3.0704740	-4.0439120	0.5086290
26	C	2.8719790	4.1608610	-0.4727660
27	C	1.8363810	0.1842500	2.0010530
28	C	2.0952900	-0.1002640	-1.9618510
29	H	-5.3856790	-3.1940940	-0.7381350
30	H	-1.1505290	-3.4627220	-0.1986110
31	H	-3.3099790	-4.5879460	-0.6255260
32	H	-5.6256290	2.9724680	0.1289350
33	H	-1.4001390	3.4214940	0.6291960
34	H	-3.6504640	4.4464750	0.5664770
35	H	0.5188260	-3.3199510	0.7263400
36	H	0.3674020	3.3849620	-0.0806220
37	H	3.5523770	-4.3859890	-0.4128480
38	H	3.8377280	-4.0311160	1.2898060
39	H	2.3085970	-4.7718700	0.7935750
40	H	3.3094900	4.2451580	-1.4726900
41	H	2.0731820	4.8988440	-0.3765990
42	H	3.6577470	4.4178310	0.2456520
43	H	2.4402760	-0.6723880	2.3004770
44	H	2.4128640	1.0938290	2.1670600
45	H	0.9440690	0.2164090	2.6285590
46	H	2.9652220	-0.1420960	-2.6171180
47	H	1.5011780	-1.0028840	-2.1168220
48	H	1.4905230	0.7646740	-2.2407750

## X. References

- 1) Ko, C.-C.; Kwok, W.-M.; Yam, V.; Phillips, D. *Chem. Eur. J.* **2006**, *12*, 5840–5848.
- 2) Ikeda, H.; Sakai, A.; Kawabe, A.; Namai, H.; Mizuno, K. *Tetrahedron Lett.* **2008**, *49*, 4972–4976.
- 3) Herder, M.; Schmidt, B. M.; Grubert, L.; Patzel, M.; Schwarz, J.; Hecht, S. *J. Am. Chem. Soc.* **2015**, *137*, 2738–2747.
- 4) Yokoyama, S.; Hirose, T.; Matsuda, K. *Langmuir* **2015**, *31*, 6404–6414.
- 5) Frath, D.; Sakano, T.; Imaizumi, Y.; Yokoyama, S.; Hirose, T.; Matsuda, K. *Chem. Eur. J.* **2015**, *21*, 11350–11358.
- 6) Herder, M.; Eisenreich, F.; Bonasera, A.; Grafl, A.; Grubert, L.; Patzel, M.; Schwarz, J.; Hecht, S. *Chem. Eur. J.* **2017**, *23*, 3743–3754.
- 7) Lvov, A. G.; Yadykov, A. V.; Lyssenko, K. A.; Heinemann, F. W.; Shirinian, V. Z.; Khusniyarov, M. M. *Org. Lett.* **2020**, *22*, 604–609.
- 8) Sumiya, Y.; Higashiguchi, K.; Matsuda, K. *Chem. Commun.* **2020**, *56*, 2447–2450.
- 9) Milek, M.; Heinemann, F. W.; Khusniyarov, M. M. *Inorg. Chem.* **2013**, *52*, 11585–11592.
- 10) SADABS, 2008/1; Bruker AXS, Inc.: Madison, WI, **2009**.
- 11) Sheldrick, G. *Acta Crystallogr., Sect. A: Found. Crystallogr.* **2008**, *64*, 112–122.
- 12) Sheldrick, G. *Acta Crystallogr., Sect. C: Struct. Chem.* **2015**, *71*, 3–8.
- 13) Herder, M.; Eisenreich, F.; Bonasera, A.; Grafl, A.; Grubert, L.; Patzel, M.; Schwarz, J.; Hecht, S. *Chem. Eur. J.* **2017**, *23*, 3743–3754.
- 14) Pommerehne, J.; Vestweber, H.; Guss, W.; Mahrt, R. F.; Bässler, H.; Porsch, M.; Daub, J. *Adv. Mater.* **1995**, *7*, 551–554.
- 15) Kahn, O. Molecular Magnetism, VCH Publishers Inc., **1993**.
- 16) Mörtel, M.; Witt, A.; Heinemann, F. W.; Bochmann, S.; Bachmann, J.; Khusniyarov, M. M. *Inorg. Chem.* **2017**, *56*, 13174–13186.
- 17) Bill, E. mf.SL package, version 2.2, MPI for Bioinorganic Chemistry, Mülheim/Ruhr, Germany.
- 18) Sumi, T.; Takagi, Y.; Yagi, A.; Morimoto, M.; Irie, M. *Chem. Commun.* **2014**, *50*, 3928–3930.
- 19) Gaussian 09, Revision A.02, M. J. Frisch, G. W. Trucks, H. B. Schlegel, G. E. Scuseria, M. A. Robb, J. R. Cheeseman, G. Scalmani, V. Barone, B. Mennucci, G. A. Petersson, H. Nakatsuji, M. Caricato, X. Li, H. P. Hratchian, A. F. Izmaylov, J. Bloino, G. Zheng, J. L. Sonnenberg, M. Hada, M. Ehara, K. Toyota, R. Fukuda, J. Hasegawa, M. Ishida, T. Nakajima, Y. Honda, O. Kitao, H. Nakai, T. Vreven, J. A. Montgomery, Jr., J. E. Peralta, F. Ogliaro, M. Bearpark, J. J. Heyd, E. Brothers, K. N. Kudin, V. N. Staroverov, R. Kobayashi, J. Normand, K. Raghavachari, A. Rendell, J. C. Burant, S. S. Iyengar, J. Tomasi, M. Cossi, N. Rega, J. M. Millam, M. Klene,

- J. E. Knox, J. B. Cross, V. Bakken, C. Adamo, J. Jaramillo, R. Gomperts, R. E. Stratmann, O. Yazyev, A. J. Austin, R. Cammi, C. Pomelli, J. W. Ochterski, R. L. Martin, K. Morokuma, V. G. Zakrzewski, G. A. Voth, P. Salvador, J. J. Dannenberg, S. Dapprich, A. D. Daniels, O. Farkas, J. B. Foresman, J. V. Ortiz, J. Cioslowski, and D. J. Fox, Gaussian, Inc., Wallingford CT, 2009.
- 20) Miertus, S.; Scrocco, E.; Tomasi, *J. Chem. Phys.* **1981**, *55*, 117–129.
  - 21) Adamo, C.; Barone, V. *J. Chem. Phys.* **1999**, *110*, 6158–6170.
  - 22) Becke, A. D. *Phys. Rev. A* **1988**, *38*, 3098–3100.
  - 23) Becke, A. *J. Chem. Phys.* **1993**, *98*, 5648–5652.
  - 24) Patel, P. D.; Masunov, A. E. *J. Phys. Chem. A* **2009**, *113*, 8409–8414.
  - 25) Zhao, Y.; Schultz, N. E.; Truhlar, D. G. *J. Chem. Theory Comput.* **2006**, *2*, 364–382.
  - 26) Casida, M.; Jamorski, C.; Casida, K.; Salahub, D. *J. Chem. Phys.* **1998**, *108*, 4439–4449.
  - 27) Zhao, Y.; Schultz, N. E.; Truhlar, D. G. *J. Chem. Phys.* **2005**, *123*, 161103.
  - 28) Yam, V. W. W.; Ko, C. C.; Zhu, N. Y. *J. Am. Chem. Soc.* **2004**, *126*, 12734–12735.